

THE OPERATING PRINCIPLES OF THE ASCARIS LUMBRICOIDES  
PHARYNX AS STUDIED BY EXPERIMENT AND MODEL ANALYSIS

By

James Richard Saunders

B.Sc., University of Victoria, 1965

A THESIS SUBMITTED IN PARTIAL FULFILLMENT OF  
THE REQUIREMENTS FOR THE DEGREE OF  
MASTER OF SCIENCE  
in the Department  
of  
Biological Sciences

© JAMES RICHARD SAUNDERS

SIMON FRASER UNIVERSITY

SEPTEMBER, 1972

APPROVAL

Name: James Richard Saunders

Degree: Master of Science

Title of Thesis: The operating principles of the Ascaris lumbricoides  
pharynx as studied by experiment and model analysis.

Examining Committee:

Chairman: G. H. Geen

---

A. H. Burr  
Senior Supervisor

---

P. Belton  
Examining Committee

---

B. L. Jones  
Examining Committee

---

E. M. Shoemaker  
Examining Committee

---

W. E. Vidaver  
Examining Committee

---

J. M. Webster  
Examining Committee

Date approved: 12 October 1972

## ABSTRACT

The operating principles of the pharynx of Ascaris lumbricoides (var. suum) were studied by experiment and model analysis. The average pharynx could be represented by two co-axial truncated cones in which the posterior end is twice the diameter of the anterior end. The ratio of the length of one ray of the triradiate lumen to the radius of the pharynx was found to be a constant,  $0.46 \pm .01$  (S.E.).

The average velocity of propagation of the membrane depolarization in the isolated pharynx was  $4.0 \pm .20$  cm/sec (S.E.) whereas the average velocity of membrane repolarization was  $5.8 \pm .23$  cm/sec (S.E.). Therefore, action potential duration progressively decreases away from the site of action potential origin. Muscle contraction resulted in localized pressure increases within the cytoplasm of the pharynx. These pressure changes were transmitted through the pharynx at a lower velocity than the action potential.

High speed cinematography revealed that for the isolated pharynx, dimensional changes during repetitive muscle contraction were primarily longitudinal. The length increased from 9% to 18% with a mean of 15% at the anterior region and was considerably less at the posterior region of the pharynx. Model analysis predicted a change in length of the anterior region consistent with a pharyngeal lumen opening of 70% of the full cross section. This is equivalent to the lumen opening to a triangular configuration.

The pharynx pumping sequence was reconstructed using the experimental values discussed above and using the in vivo pumping rate (4 pumps/sec compared with 2.5 pumps/sec maximum in the isolated pharynx). A physically realistic peristaltic motion of the model lumen resulted when the pacesetter region for sequential pumping was assumed to be at the anterior end of the pharynx.

A mathematical model of the pharynx was constructed using the Membrane Theory of Shells. The circumferential strain to longitudinal strain ratio ( $\epsilon_{\psi}/\epsilon_{\ell}$ ) was calculated for various pressure stresses on the pharynx and compared to experimentally determined values.

$\epsilon_{\psi}/\epsilon_{\ell}$  was found to be 0.73 by stressing the pharynx passively by osmotic pressure, indicating that the pharynx membrane is heterogeneous and the ratio of circumferential to longitudinal elastic constants,  $E_{\psi}/E_{\ell} \approx 2.7$ .

$\epsilon_{\psi}/\epsilon_{\ell}$  was predicted to be 0.41 to 0.54 for very slow opening of the lumen (the equilibrium condition). An experimental value obtained for maintained muscle contraction was  $\epsilon_{\psi}/\epsilon_{\ell} = 0.46 \pm .1$ .

The negligible, or very small positive or negative, radial strains during repetitive pumping were consistent with the myofilament force per unit area being approximately 100% in excess of pharynx pressure.

It was shown that the ratio of pharyngeal volume to nematode volume was limited, especially in nematodes over 100 mm in total length. The advantage of increased pharyngeal efficiency because of the decreasing pharynx/nematode volume ratio is discussed.

## ACKNOWLEDGEMENTS

I would like to begin this acknowledgement by expressing thanks in general to all of my fellow students and to the faculty of the Biology and Physics Departments for the discussion, criticism, and encouragement which added greatly to this project.

Special thanks must go to Dr. A. H. Burr for taking me in as a student and guiding me through two years of study. His gift of asking incisive questions contributed immensely to the final report.

I am grateful to Dr. P. Belton for introducing me to electrophysiology and for acting as a consultant on many "artifacts".

I wish to thank Swift's Canadian Company for the use of their facilities, and Dr. J. Rusko for his assistance in making arrangements for the collection of samples.

Thanks are due to R. Paulson for his assistance in developing the fixation embedding procedures used in this study.

And finally to my wife, Darlene, for her forbearance, and contribution by typing many drafts.

## TABLE OF CONTENTS

	Page
Examining Committee Approval .....	ii
Abstract .....	iii
Acknowledgements .....	v
Table of Contents .....	vi
List of Tables .....	viii
List of Figures .....	ix
CHAPTER 1. Introduction .....	1
CHAPTER 2. Materials and Methods .....	10
A. Collection and Storage .....	10
B. Dissection .....	12
C. Experimental Chamber .....	12
D. Electrophysiology - Electrodes .....	17
E. Electronics .....	17
F. Fixation and Embedding .....	20
CHAPTER 3. The Pumping Sequence .....	23
A. Average Dimensions of the Pharynx .....	23
1. External dimensions .....	23
2. Internal dimensions .....	26
B. High Speed Cinematography of the Isolated Pumping Pharynx .....	26
1. Methods .....	26
2. Results .....	27
C. Propagation Velocity of the Electrical Activity in the Isolated Pharynx .....	36
1. Methods .....	36
2. Results and Discussion .....	39
a) Differences in depolarization and repolarization velocities .....	42
b) Velocity as a function of position along pharynx .....	43
c) Factors contributing to the variation in velocity .....	43
d) Some observations on the electro- physiology of the pharynx membrane .	45

	Page
D. Pressure Changes Within the Isolated Pharynx During Pumping .....	46
1. Method .....	46
2. Results and Discussion .....	46
E. <u>In vivo</u> Pumping Parameters - Summary of Work Done by C. Mapes .....	52
F. Reconstruction of the Pumping Sequence .....	53
G. Forces Acting on the Lumen Contents .....	56
H. Discussion and Conclusion .....	59
 CHAPTER 4. The Model Pharynx .....	 63
A. Changes in Dimensions Induced by Osmotic Stress .....	63
1. Method .....	63
2. Results .....	64
3. Discussion .....	67
B. The Model Pharynx .....	68
1. Assumptions and definitions .....	68
2. Conditions for opening the lumen .....	72
3. Myofilament force per unit area .....	75
4. The relationship between R, $\ell$ , and r .....	76
5. Normal opening of lumen .....	77
6. The relationship between stress, strain, and myofilament force .....	80
a) Theory and definitions .....	80
b) Simple conical pressure cylinder .....	83
c) Model pharynx, very slow opening of lumen .....	84
d) Model pharynx, sequential opening of lumen .....	86
C. Size, Shape, and Efficiency .....	89
1. Maximum diameter of pharynx .....	89
2. Limitation to pharynx length .....	89
3. Efficiency and the elongating pharynx ...	92
4. The tapered pharynx .....	95
 CHAPTER 5. Discussions and Conclusion .....	 98
A. General Discussion .....	98
B. Future Extensions of this Work .....	99
C. Conclusions .....	100
 Bibliography .....	 103
 Curriculum Vitae .....	 107

LIST OF TABLES

	Page
Table 2-1	
Ionic composition of solutions used for storage of <u>Ascaris</u> and for <u>in vitro</u> work with <u>Ascaris</u> pharynx..	11
Table 4-1	
Value of the strain/strain ratio ( $\epsilon_{\psi}/\epsilon_{\ell}$ ) for three values of lumen radius during very slow opening of pharyngeal lumen.....	86



## LIST OF FIGURES

		Page
Figure 1-1	Generalized diagram of anterior end of nematode.	4
Figure 1-2	Photomicrographs of <u>Ascaris</u> pharynx.	6
Figure 2-1	Diagram of constant temperature chamber.	14
Figure 2-2	Electrode configuration for the determination of the velocity of electrical activity.	16
Figure 2-3	Schematic diagram of electrode testing circuit and simultaneous stimulate-record circuit.	19
Figure 3-1	The average external diameter of the pharynx as a function of position.	25
Figure 3-2	Relative length of the posterior 4/5 of a pharynx as a function of time.	29
Figure 3-3	Relative length of anterior and posterior regions of pharynx as a function of time.	31
Figure 3-4	Relative change in dimensions as a function of time for a single pharynx in which myofilament relaxation failed to occur.	33

		Page
Figure 3-5	Electrical activity of pharynx, recorded with internal electrodes.	35
Figure 3-6	Circuit block diagram of apparatus used in the action potential velocity experiments.	38
Figure 3-7	Externally recorded electrical activity of the pharynx.	41
Figure 3-8	Circuit block diagram of apparatus used to detect electrical activity and pharynx pressure changes during myofilament contraction.	48
Figure 3-9	Simultaneous record of externally recorded electrical events and pressure changes during myofilament contraction.	50
Figure 3-10	Reconstruction of the pumping sequence.	55
Figure 4-1	Relative change in radius versus the relative change in length caused by osmotic stress.	66
Figure 4-2	Schematic diagram of model pharynx.	70
Figure 4-3	Schematic cross section of pharynx.	73

	Page
Figure 4-4	Relative change in length versus relative change in radius for two degrees of lumen dilation, as calculated from equation 4-11. 79
Figure 4-5	Diameter of pharynx as a function of the diameter of the nematode, after Roggen (1970). 91
Figure 4-6	Pharynx length as a function of nematode length. 94

## CHAPTER 1

### INTRODUCTION

The objective of this study was to investigate further the operating principles of the nematode pharynx, by studying the mechanical, electrical, and pressure changes during the pumping sequence. Also, as a major part of this work, to incorporate these data into a mathematical model of the pharynx.

Ascaris lumbricoides was chosen for study because of its large size and ready availability. Also pharynx symmetry and lack of specializations such as median bulbs in this animal made the mathematics less complex than would have been possible for some other species.

Nematodes, or round worms, are animals with a large length to diameter ratio (approximately 50:1 in adult Ascaris). There is a large variation in body size, extending from less than 1 millimeter in most free living nematodes to over 500 millimeters in some parasitic species (200-300 mm was the typical size of Ascaris females collected). The body shape is of two general types, cylindrical (filiform) or spindle-shaped (fusiform) as in Ascaris.

The nematode body wall is composed of a multilayer cuticle, the hypodermis and a layer of longitudinally oriented somatic muscle cells. In Ascaris, each mononucleated muscle cell has three parts:

a) a spindle-shaped fiber parallel to the long axis of the worm (del Castillo, de Mello and Morales, 1967), containing obliquely striated muscle (Rosenbluth, 1967);

b) at the mid-point of the spindle, the cell expands into a large bag (up to 600  $\mu$  in diameter) called the muscle "belly";

c) a cylindrical arm that extends from the junction of the muscle fiber and muscle belly, to the nerve cord. Each arm divides into fingers which inter-lace with fingers of adjacent arms to form a muscle syncytium in close proximity with the nerve cord (del Castillo, de Mello and Morales, 1967).

The somatic musculature is always under tonus, maintaining the body cavity (pseudocoelom) at an average pressure of 70 mm Hg (range 25-225 mm of Hg as measured by Harris and Crofton, 1957).

The nematode alimentary canal may be divided into three parts:

a) stomodaeum, includes mouth, lips, buccal cavity and pharynx (esophagus)

b) intestine

c) proctodaeum, rectum and anus in females and cloaca in males.

The only motile segment of the canal is the pharynx, a muscular and glandular pumping organ with a triradiate lumen (Figs. 1-1 and 1-2).

There is considerable variability in the shape of the pharynx. Allen (1960) considered three general subdivisions:

a) one-part cylindrical form as in Ascaris (Fig. 4-2).

b) two-part cylindrical form in which there is a slender anterior non-muscular part and swollen, glandular and muscular posterior part.

c) three-part cylindrical form containing corpus, isthmus and bulb regions.

Fig. 1-1

Generalized diagram of the anterior region of  
a nematode.

BC - buccal cavity

C - cuticle

I - intestine

L - lumen

LP - lips

NR - nerve ring

P - pharynx

PC - pseudocoelom

PIV - pharyngo-intestinal valve

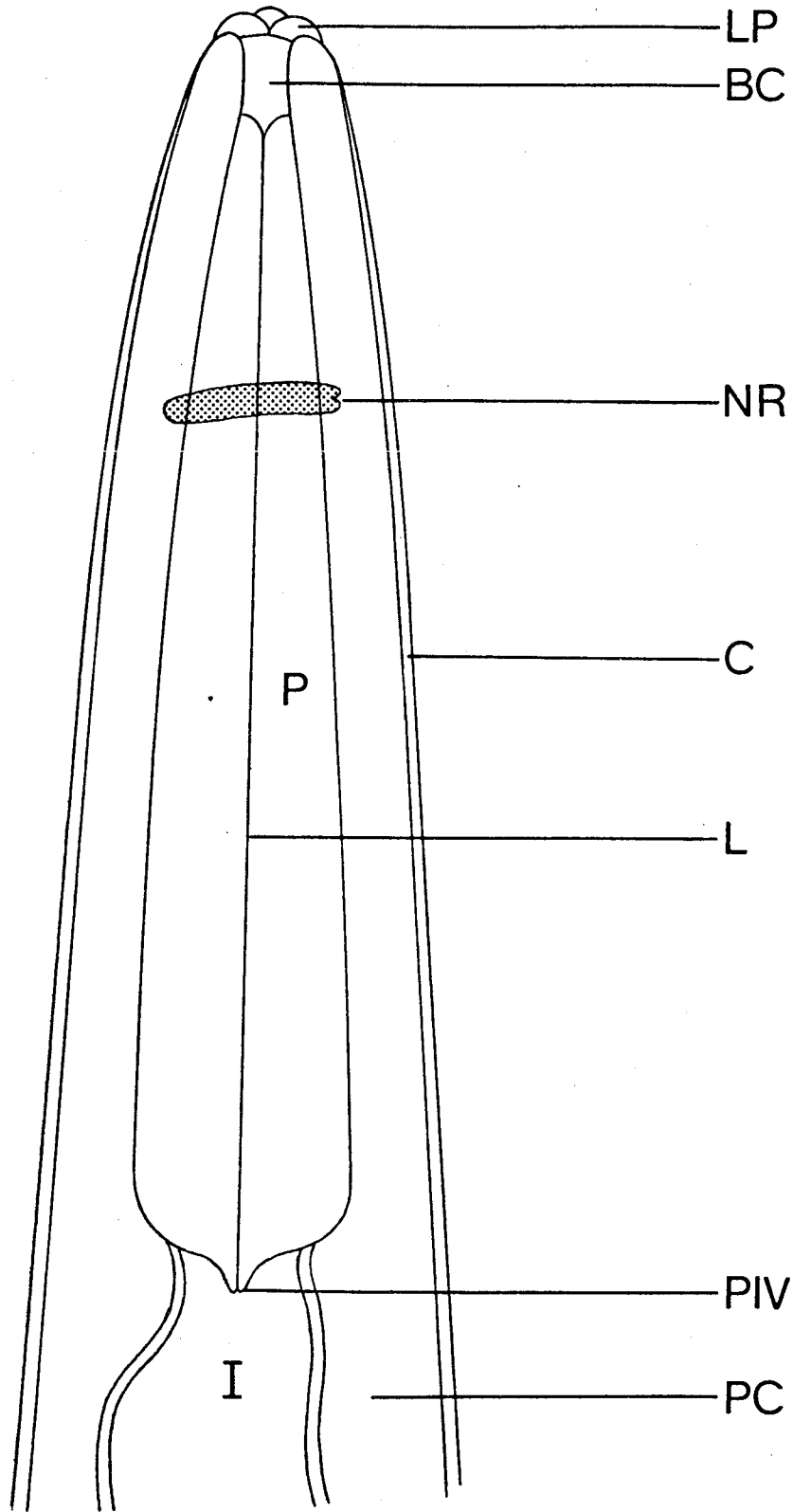


Fig. 1-2

- A. transverse section through anterior region of pharynx (X 200) showing the lumen open to the triangular configuration.
- B. transverse section through the pharynx in the posterior region (X 150) showing the triradiate lumen and tricuspid, pharyngo-intestinal valve.

BW - body wall

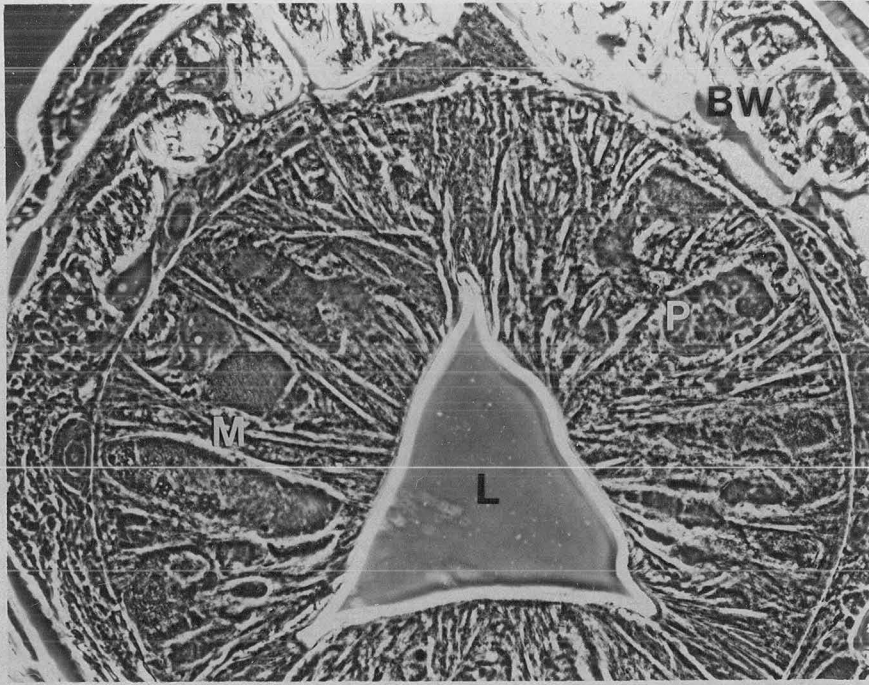
M - radial myofilaments

L - lumen

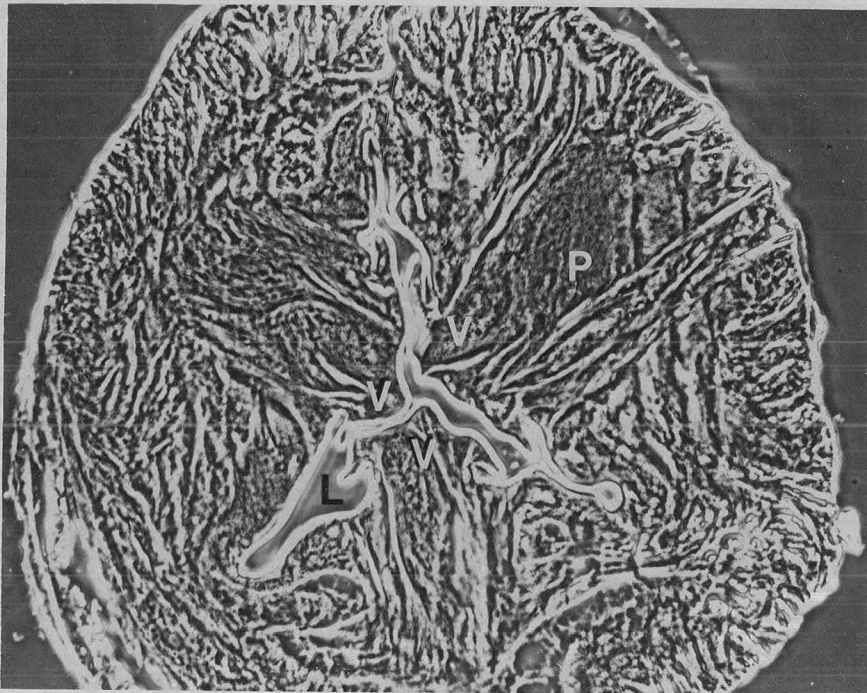
P - pharynx cytoplasm

V - tricuspid valve





A



B

The radially oriented, non-striated, myofilaments (Reger, 1966) are the only contractile elements of the pharynx (Chitwood and Chitwood, 1950). Muscle contraction dilates the lumen and ingests food (a liquid or liquid and particulate matter as Ascaris inhabits the small intestine of pig or man). The lumen closes on muscle relaxation and food is pumped into the intestine.

The intestine is a flaccid tube which is normally collapsed by the pseudocoelom pressure. The pharynx must raise the pressure of the lumen contents above that of the pseudocoelom to fill the intestine. Thus the pharynx is a pressure pump and in Ascaris, an efficient one, as no regurgitation of lumen contents is observed during pumping (Mapes, 1966).

The nervous system of Ascaris consists of four main longitudinal nerve cords; mid-dorsal, mid-ventral, and a pair of laterals. There are also subventral and subdorsal nerve cords and numerous commissures. A nerve ring, encircling the pharynx, is located approximately one-fourth of the pharynx length back from the anterior end. The nerve ring and the ganglia close to it can be considered the central nervous system of this animal (Bullock and Holmes, 1965).

The axons innervating the somatic muscle are cholinergic, but apparently the choline ester is a neuro-hormone and not a nerve-muscle transmitter. The somatic muscles are myogenic (spontaneously active), the choline ester released by the nerve junctions controls the state of polarization of the muscle syncytium, and thereby controls, via the

"arm" of the muscle cell, the rate of myogenic activity (del Castillo, de Mello and Morales, 1963 and 1967).

Two enteric nervous systems are known, one in the pharyngeal and one in the rectal region. The pharynx has three longitudinal nerves, one dorsal and two sub-ventral, which extend almost the full length within the pharynx. Two or possibly three commissures join the longitudinal cords together. The enteric nervous system of the pharynx connects with the ventral segment of the circumferential nerve ring (Bullock and Holmes, 1965).

Considerable work has been done on the electrophysiology of the pharynx muscle of Ascaris by del Castillo and his co-workers (del Castillo and Morales, 1967a and 1967b; and del Castillo, de Mello and Morales, 1964). The pharynx membrane has a normal resting potential of -38 mV in natural perientric fluid and -34 mV in artificial perientric fluid (APF). The magnitude of the potential difference is related to the concentration of chloride in the extracellular fluid. Spontaneous membrane activity or electrical stimulation trigger a depolarization with an over-shoot of 17 mV. Spontaneous repolarization proceeds via a potassium phase, and as the potassium equilibrium potential is negative to the resting potential, a marked hyper-polarization is produced (Fig. 3-5 A).

The membrane shows spontaneous subthreshold activity in both polarized and depolarized states (for example, see: Fig.3-5A and 3-5B, and del Castillo and Morales, 1967a).

Similar to other membranes (Kobatake, Tasaki and Watanake, 1971) the pharynx muscle has two stable states. It may be stimulated from the normal resting potential or, if depolarized (by an excess of  $Cl^-$  in the extracellular fluid) the muscle may be stimulated to produce an action potential that is entirely negative going. In artificial perienteric fluid, the pharynx occasionally pauses or sticks in the contracted state with a membrane potential of zero. Relaxation can be initiated by electrical stimulation (del Castillo and Morales, 1967a).

Little work has been done on the functional physiology of the pharynx. Martini, (1916) on the basis of anatomical studies on Oxyuris curvula discussed the mechanical properties of the pharynx. His arguments were based on a two dimensional model of the pharynx expanding radially. (I found it necessary to use a three dimensional model to explain the radial and longitudinal expansion of the pharynx of Ascaris.) Mapes, (1966) did one experiment in which he observed the volume of fluid imbibed versus time by Ascaris. On the basis of this experiment and anatomical studies (Mapes, 1965), Mapes speculated on the operating principles of the pharynx. Some of his basic premises were incorrect however, as will be pointed out in this report.

## CHAPTER 2

### MATERIALS AND METHODS

#### A. Collection and storage

Nematodes were collected from the small intestine of freshly killed pigs and placed in a thermos bottle containing 30% artificial seawater (ASW) (Hobson, Stephanson and Beadle, 1952; and del Castillo and T. Morales, 1969) and 1 g/liter glucose at 38°C (Table 2-1). The addition of glucose seemed to keep the worms in better condition.

At the laboratory, worms were transferred to fresh 30% ASW+glucose and stored (6-12 worms per 16 oz. jar) at 36-38°C during the day and 30-32°C at night. The practice of lowering the storage temperature and in addition, changing the storage solution twice per day, kept the nematodes in good condition (active movements and active muscle preparations) for 3-4 days. Most experiments were completed within 36 hours of collection, however, to avoid artifacts caused by starvation. Another precaution taken was to store the nematodes in the dark, as there are references in the literature, but no experimental evidence, of Ascaris being sensitive to light (del Castillo and Morales, 1969).

All experiments on the pharynx muscle were done under artificial perientric fluid (APF) as formulated by del Castillo and Morales (1969), except that isothionate ion was substituted for acetate because acetate is postulated to be an intermediate of the modified glycolytic pathway in Ascaris (Lee, 1965). The excess acetate may have influenced the electrical activity of the membrane.

Table 2-1. Ionic composition of solutions used for storage of Ascaris and in vitro work with Ascaris pharynx.

	Isothio-				Trizma			Acetic					
	Na <sup>+</sup> mM	K <sup>+</sup> mM	Ca <sup>++</sup> mM	Mg <sup>++</sup> mM	Cl <sup>-</sup> mM	Acetate mM	nate mM	OH <sup>-</sup> mM	HCO <sub>3</sub> <sup>-</sup> mM	base mM	Sucrose mM	acid to PH=7	Glucose mM
APF (Acetate)	129.0	24.5	5.9	4.9	50.0	125.1	-	-	-	-	7.5	-	-
APF (Isothio- nate)	129.0	24.5	5.9	4.9	50.0	-	125.1	-	-	-	7.5	-	-
APF (Acetate Buffered)	129.0	24.5	5.9	4.9	50.0	125.1	-	-	-	7.5	-	✓	-
30% Seawater	135.8	3.0	3.0	15.9	175.4	-	-	-	0.8	-	-	-	-
30% Seawater + 1 g/l glucose	135.8	3.0	3.0	15.9	175.4	-	-	-	0.8	-	-	-	5.5
Kronecker's Solution	158.9	-	-	-	157.4	-	-	1.5	-	-	-	-	-

## B. Dissection

The pharynx was dissected out by cutting off the anterior 2-3 cm of the worm and pinning the section, through the body wall and intestine, to a paraffin block with a 000 size insect pin. The section was covered with APF and a cut was made with scissors along one of the lateral lines to within less than 1 mm of the lips. The body wall was carefully pulled away from the pharynx and pinned. The radial elastic support fibers connecting pharynx and somatic musculature were severed using scissors and a dissecting pin. Special care was taken to avoid damaging the outer pharyngeal membrane by tearing and internal pharyngeal membranes by stretching of the pharynx. The freed body wall was cut off circumferentially 1.0-1.5 mm from the anterior and discarded.

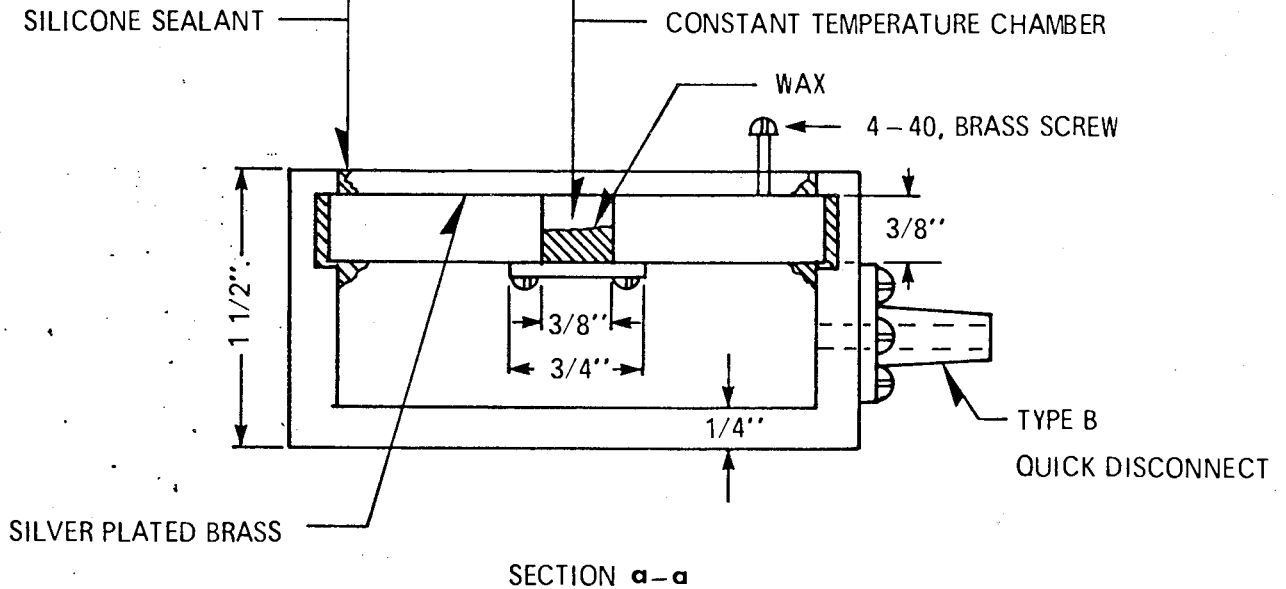
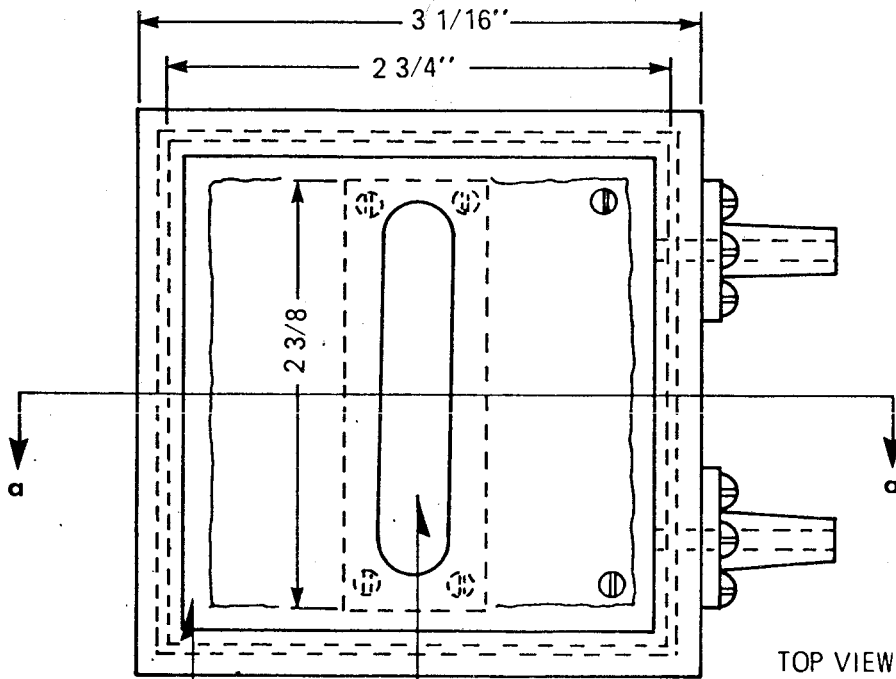
## C. Experimental Chamber

The pharynges were placed one at a time in a chamber (Fig. 2-1) with the temperature regulated by water circulated from a Haake constant temperature bath. The silver coated brass plate served as an efficient heat conductor and as the reference electrode in electrophysiological measurement. For velocity and pressure measurements an electrode apparatus (Fig. 2-2) was used inside the chamber but for all other experiments the chamber was half filled with black paraffin to which the pharynx could be pinned.

Fig. 2-1

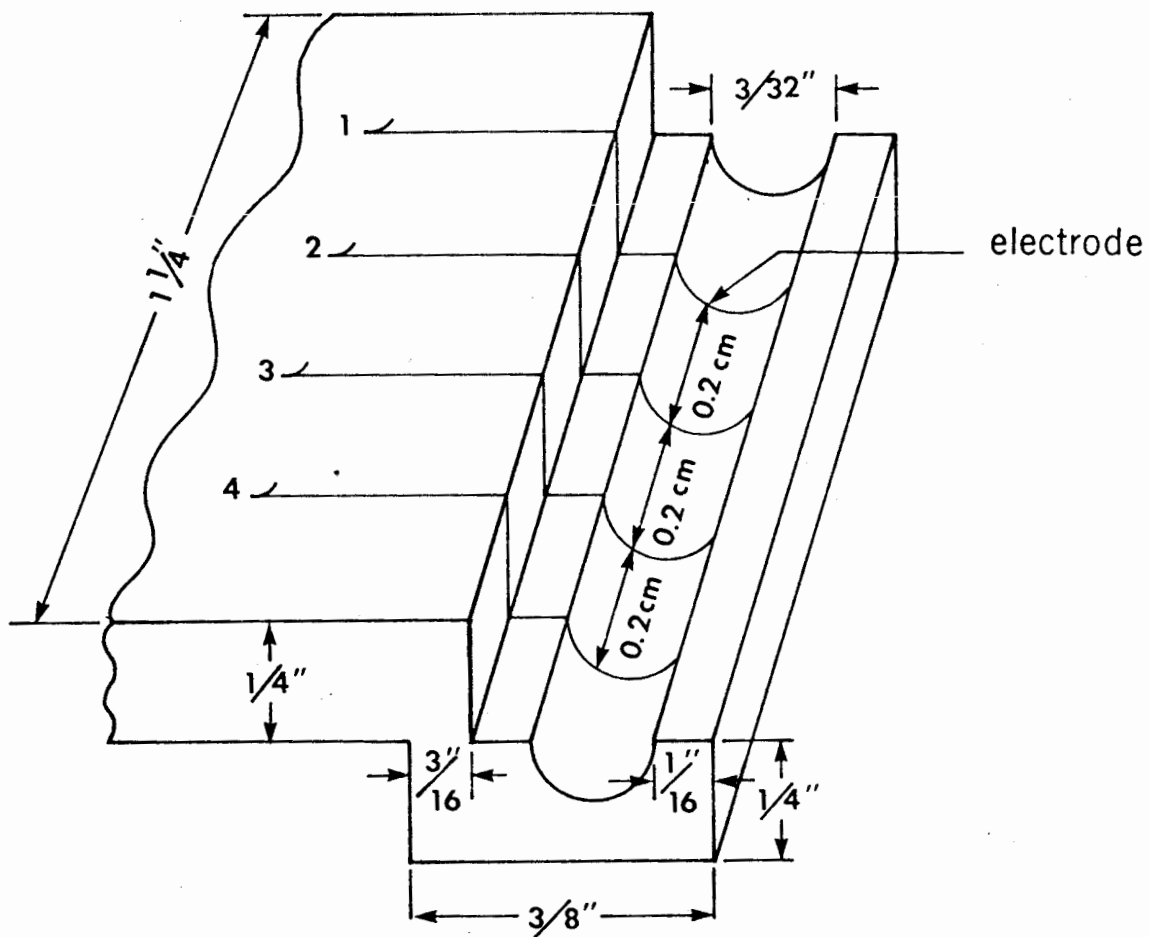
Diagram of constant temperature chamber used  
for all experimental work.





MATERIAL:  
ALL PLEXIGLASS, EXCEPT FOR BRASS PLATE

Fig. 2-2            Electrode apparatus used in the external  
detection of pharyngeal electrical activity  
during pumping. The 0.005 inch wires 1, 2, 3  
and 4 go to preamplifiers as shown in  
Fig. 3-6.



MATERIAL : PLEXIGLASS

#### D. Electrophysiology - Electrodes

Glass microelectrodes were pulled using a David Kopf Instruments 700B vertical pipette puller from 0.75 - 1.6 mm glass tubing. The electrode tip was inspected for imperfections and then filled with 3M KCl by the distillation method (Tasaki, Polley and Orrego, 1954). The electrodes were tested for resistance using the circuit shown in Fig. 2-3, test position.

Stainless steel electrodes were made by electrolysis (Bûres, Petran and Zachar, 1960) from number 000 insect pins, and inspected for smooth sharp points. Steel electrodes were coated using a clock drive to pull the electrodes from Varathane at a speed of about 8 cm/hr. The coating was dried for 45 min. at 45-50°C. This was repeated to give a total of three coats. The electrode coating was tested by making the electrode the anode of an electrolytic circuit. Electrodes were chosen if bubbles appeared only at the tip of the electrode.

#### E. Electronics

The electronics used in this study were commercial components (manufacturer and model number are referred to in the text) with the exception of bridge circuit (Fig. 2-3) for recording and stimulating through the same electrode.

This circuit consists of three functional units. With  $S_1$  in the "test" position,  $S_2$  applies 1 volt across the left-hand side of the bridge to measure electrode resistance. A 1 millivolt signal is detected at A, for each megohm of electrode resistance.

Fig. 2-3

Schematic diagram of the electrode testing circuit and the simultaneous stimulate-record bridge.

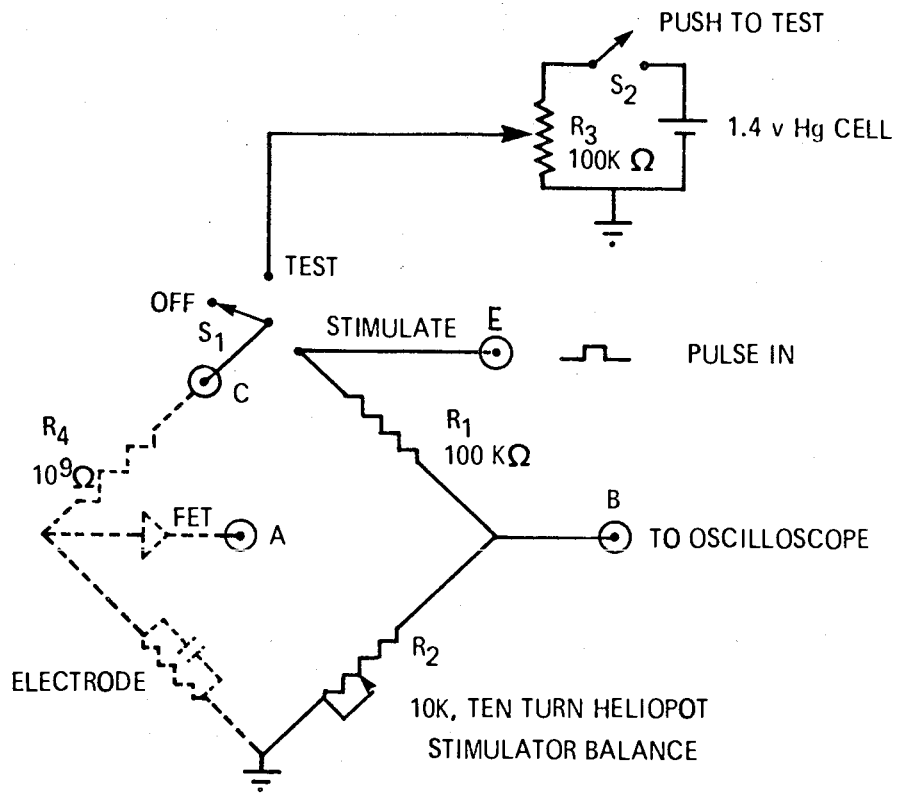
a) electrode testing

- i set  $S_1$  to test
- ii adjust  $R_3$  for 1.0 volt potential difference
- iii close  $S_2$  and a 1.0 mv signal per megohm of electrode resistance is observed at A.

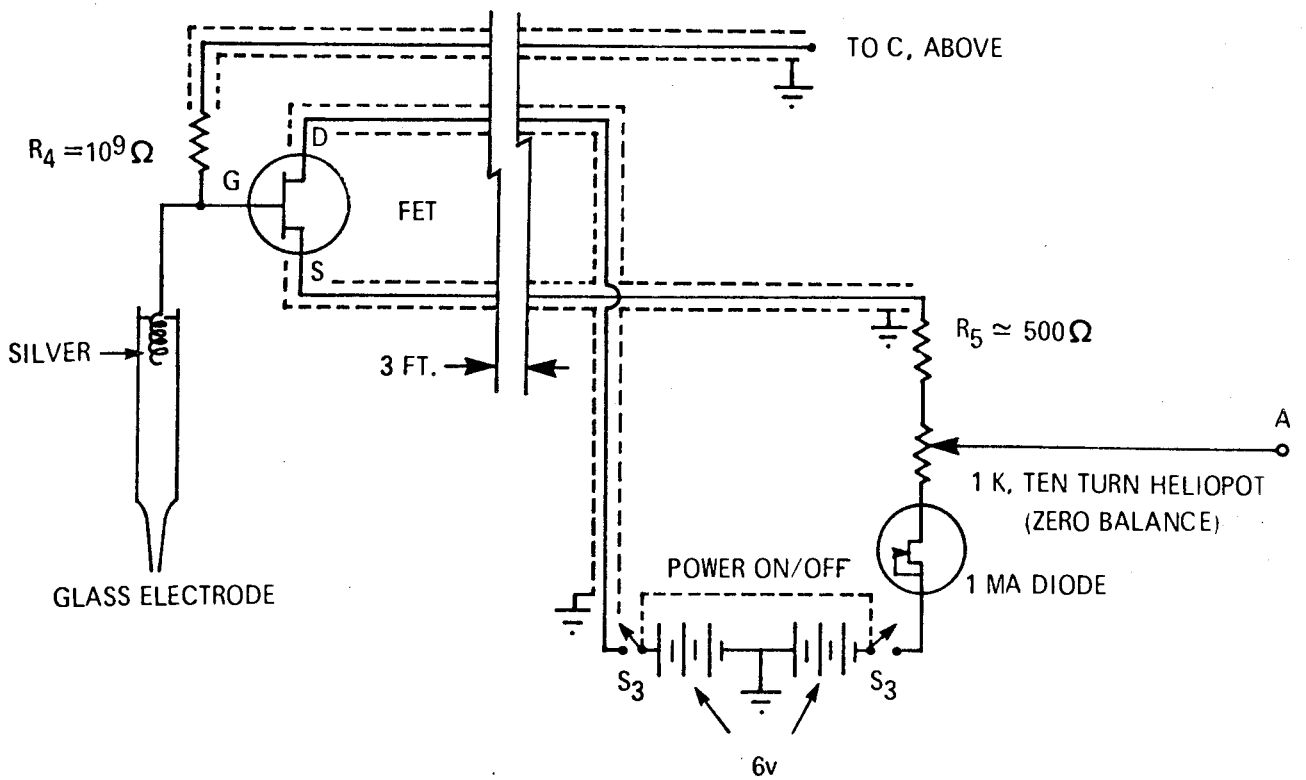
b) recording - electrical activity is detected for all positions of  $S_1$ , provided the FET power is on; switch  $S_3$ .

c) stimulate

- i set  $S_1$  to stimulate
- ii apply pulse in
- iii balance  $R_2$  for zero deflection on oscilloscope (A-B) during stimulation (on-off artifacts are observed).



BRIDGE CIRCUIT



FET PROBE CIRCUIT

With  $S_1$  in the stimulate position, a stimulus pulse applied at E may be balanced with  $R_2$ , in order that only artifacts are observed on the differential output A-B.

The field effect transistor (FET) probe circuit below is a detailed circuit of the left hand side of the bridge. The circuit was used for internal recording of the membrane potentials and action potentials, and also for checking electrode resistance. However, the pharynx could not be stimulated with this apparatus because the series  $10^9 \Omega$  resistor caused too great a voltage drop. For stimulation, a separate electrode, internal or external, was used in conjunction with an isolator circuit.

#### F. Fixation and Embedding

##### 1. Serial sections embedded in paraffin

The pharynx was dissected free of the body wall and placed in 2% glutaraldehyde in 15% seawater (osmolarity approximately 300 milliosmoles) at  $5^\circ\text{C}$  for three hours. The pharynx was dehydrated and cleared as follows:

- a) 30% ethanol, 2 hours or overnight
- b) 50% ethanol, 45 minutes
- c) 70% ethanol, 45 minutes
- d) 95% ethanol, two stages of 45 minutes each
- e) 100% ethanol, two stages of 45 minutes each
- f) xylene, two stages, 1 hour each
- g) embed in  $55^\circ\text{C}$  wax, two stages, 1 1/2 hours each.

Serial transverse sections, 10  $\mu$  thick were taken with a Spencer 820 microtome. The sections were stretched on water at 49-50°C, and placed on albuminized slides. The wax was removed with xylene and the sections mounted, unstained, in Permount. This procedure worked well for determination of the ratio of triradiate ray length to pharynx diameter. There was some shrinkage and only minimal distortion.

The attempts to obtain longitudinal sections of the wax embedded pharynx were frustrated by tearing of the sections along the lumen.

It was not possible to make serial sections of the whole anterior sections which had been prepared by the above technique because the thick cuticle prevented good embedding.

## 2. Sections embedded in plastic

To avoid the problems discussed above, the following procedure was devised to produce 3-4  $\mu$  undistorted longitudinal and transverse sections:

- a) then anterior 4-5 cm of a whole, newly collected worm was frozen in isopentane which had been cooled to the freezing point in liquid nitrogen.
- b) the end was broken off and transferred to anhydrous methanol, which had been pre-cooled in a bath of dry-ice and acetone.

The specimens were:

- c) dehydrated by daily changes of methanol, pre-cooled to dry-ice temperature, for a period of 2 weeks.
- d) fixed in 10% acrolein in xylene for 6 hours. The fixation medium was pre-cooled to dry-ice temperature and allowed to warm slowly to room temperature.



- e) transferred to fresh xylene, the excess acrolein was allowed to evaporate overnight.
- f) placed under vacuum (27 inches of water) to withdraw air bubbles.
- g) transferred to butanol overnight.
- h) transferred through a graded series to 100% glycol methacrylate and kept at 100% for approximately 2 months.
- i) polymerized, at 60°C overnight.

One to three micron transverse sections and longitudinal sections were taken with a Porter-Blum MT-1 ultramicrotome. The sections were stained with toluidine blue and mounted in Permount.

## CHAPTER 3

### THE PUMPING SEQUENCE

It was not possible to observe directly the pumping of fluid by the pharynx of Ascaris because of the opacity of the body wall and pharynx.

Therefore, the pumping sequence was reconstructed from:

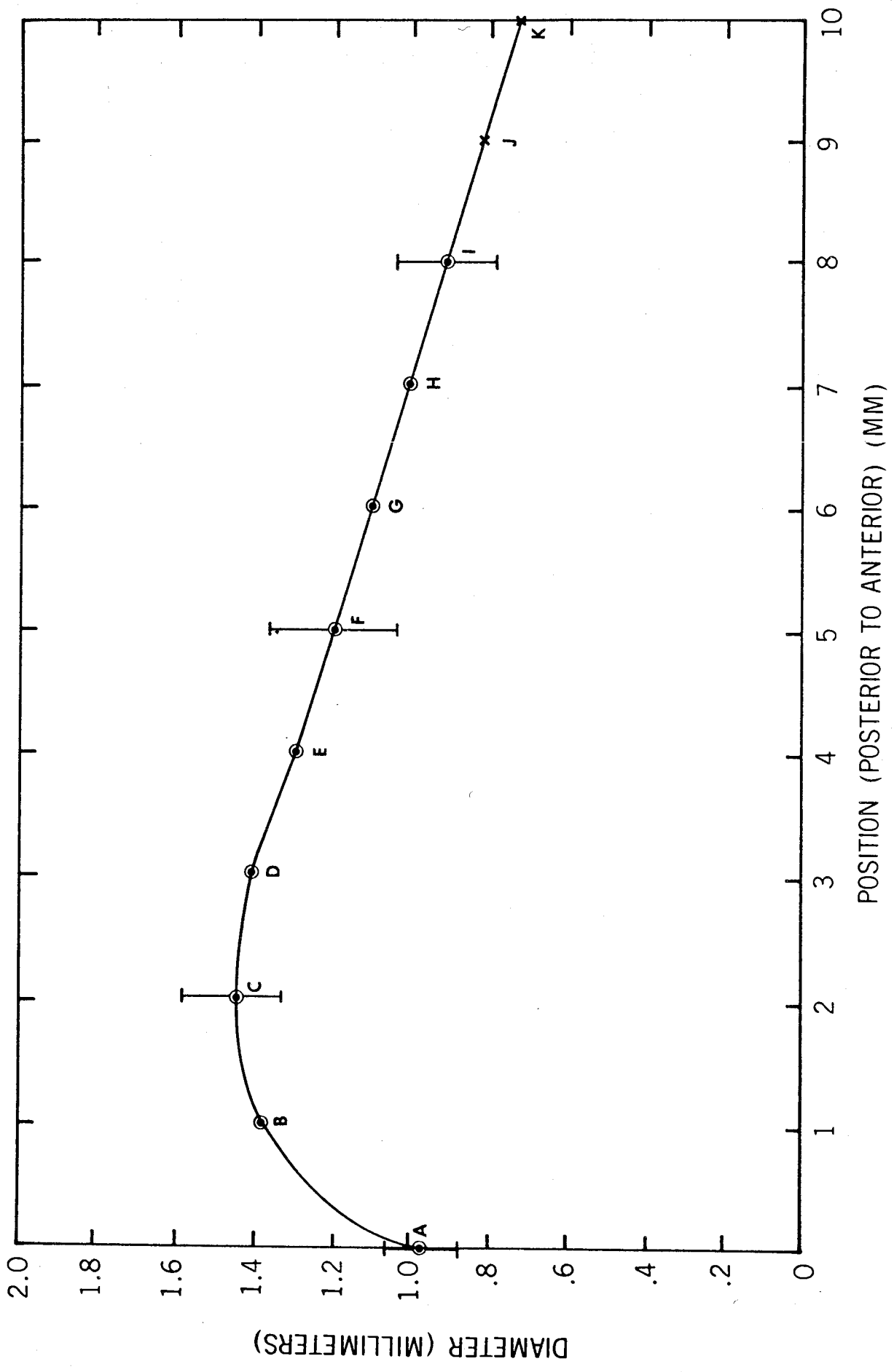
- A. the static dimensions of the pharynx as determined by serial sections and external measurements.
- B. changes in the external dimensions during pumping as measured by high speed cinematography.
- C. the propagation velocity of electrical activity in the isolated pharynx measured with external electrodes.
- D. pressure changes within the pharynx muscle during pumping which were determined with an indentation pressure guage.
- E. the rate of imbibation of fluid in vivo as determined by Mapes (1966).

#### A. Average Dimensions of the Pharynx

##### 1. External dimensions

The shape of an average pharynx was obtained by measuring twenty whole pharynges having a range of lengths from 5.5 mm to 8.6 mm (average length 7.5 mm). For each pharynx, the diameter was measured at millimeter intervals along its length, multiplied by a scale factor to normalize the dimensions to a 10 mm length, and plotted on graph paper. A best-fit smooth curve was drawn through the data points and the scaled diameter was readoff at each millimeter of length. This procedure, which resulted in nine scaled diameters  $A_1, B_1, \dots, I_1$ , was repeated for nineteen other pharynges. The data points  $A_1$  through  $A_{20}$  were averaged and plotted (Fig. 3-1, data point A). Similarly, scaled

Fig. 3-1            The mean external diameter as a function of position of twenty relaxed pharynges of original length 5.5 to 8.6 mm, scaled to 10 mm. The uncertainty bars represent plus or minus the standard deviation of the mean scaled diameter.



diameters at positions B through I were averaged and the results plotted. Points J and K (Fig. 3-1) could not be obtained directly because a few millimeters of the anterior body wall were still attached. Therefore, the curve was extended on the basis of evidence obtained from serial sections on other pharynges.

## 2. Internal dimensions

By measuring 15 photographs of the serial sections obtained by wax embedding, it was found that the ratio:

$$\alpha = \frac{x}{R} = 0.46 \pm .01 \quad (3-1)$$

where

x = the triradiate ray length (Fig. 4-3)

R = the pharynx radius

and the uncertainty shown is a standard error.

## B. High Speed Cinematography of the Isolated Pumping Pharynx

The mechanical events that occur during a pumping sequence (principally a length change) were studied using high speed cinematography.

### 1. Methods

The pharynx was removed from the nematode and placed in the constant temperature bath as described in Chapter 2. During stimulated and spontaneous activity, the pharynx was filmed at 50 frames per second with a Beulieu 2008S camera using S0-105 super 8 Extrachrome film. The film was analyzed using a Kodak model MFS-8 projector with single frame advance.

## 2. Results

Muscle contraction (shortening of radially oriented myofilaments) was detected as a change in the external dimensions of the pharynx. The changes during repetitive pumping were primarily longitudinal (Fig. 3-2) and in the anterior region of the exposed pharynx the increase was found to vary from 9% to 18% (mean of 8 measurements, 15%). The length increase in the posterior region of the exposed pharynx was much less (Fig. 3-3). The changes in radial dimensions were small during repetitive pumping (usually much less than 2%) and they were observed to be positive or negative depending on the preparation.

Muscle contraction was not always followed by immediate relaxation (Fig. 3-4). The initial rapid dimensional changes (+ 15% longitudinal and - 2.5% radial) in the first 0.08 sec were similar to those observed during repetitive pumping. Hence this was called the primary contraction phase. However, between 0.08 sec and 0.12 sec there were further dimensional changes in the pharynx (the secondary contraction phase). It was shown in chapter 4 that these additional changes were caused by equilization of pharynx stress, and by continued shortening of the radial myofilaments (beyond the length observed during repetitive pumping).

The final values of 13% length increase and 6% radial increase can be maintained for a time interval equivalent to several normal pumping periods (Fig. 3-5). Over longer periods of time however, there is a slow exponential decrease in pharynx dimensions until relaxation is initiated. The decrease in dimensions parallels an exponential decrease in pharynx pressure and an exponential repolarization of the pharynx membrane, (Fig. 3-5B).

Fig. 3-2            Relative change in length ( $l/l_0$ ) as a function  
of time determined by high speed cinematography for  
the posterior 4/5 of a single pharynx during repetitive  
pumping (2.3 pumps/second).

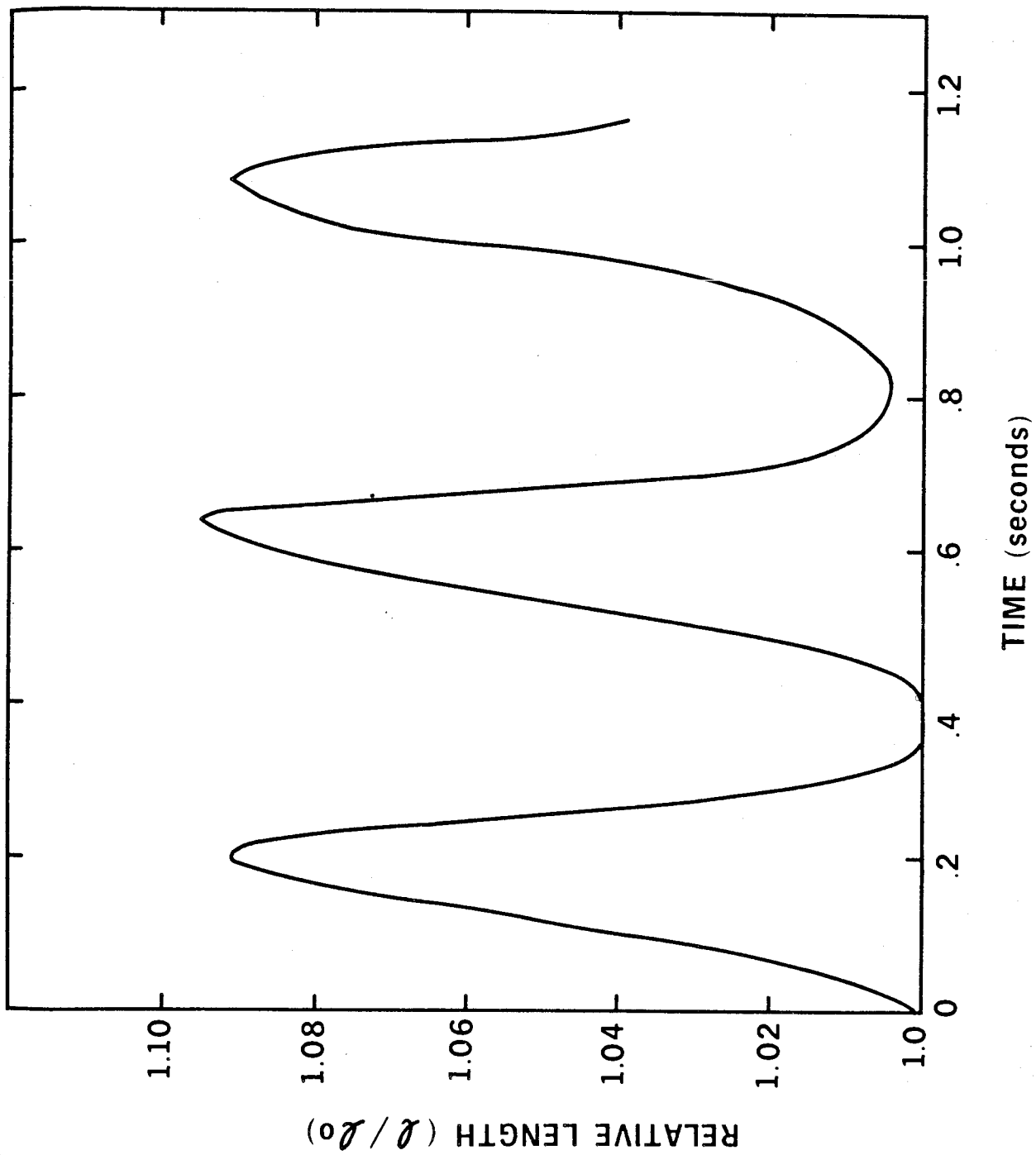




Fig. 3-3

Relative change in length of one pharynx as a function of time during repetitive pumping. Curve A: the anterior half of the pharynx exposed by dissection. Curve B: the posterior half of the exposed pharynx, including the region of the pharyngo-intestinal valve.

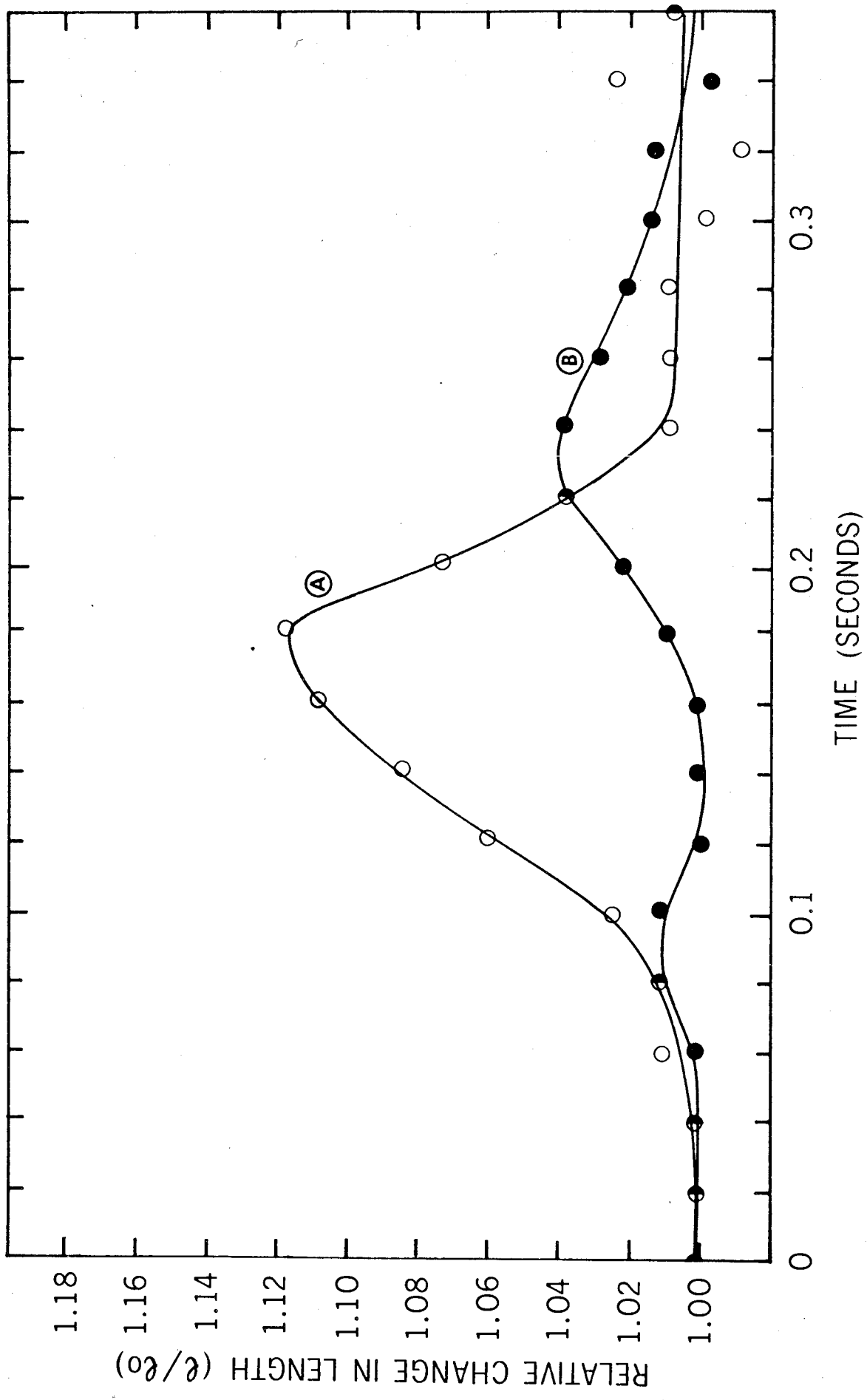


Fig. 3-4

Relative change in external dimension as a function of time for a single pharynx in which contraction was initiated but relaxation failed to occur. The sequence was considered to be comprised of a primary phase - rapid muscle contraction, and a secondary phase - stress equilization and further muscle contraction.

$l/l_0$ , relative length

$R/R_0$ , relative radius

The uncertainty bars are estimated uncertainties for taking a single measurement.

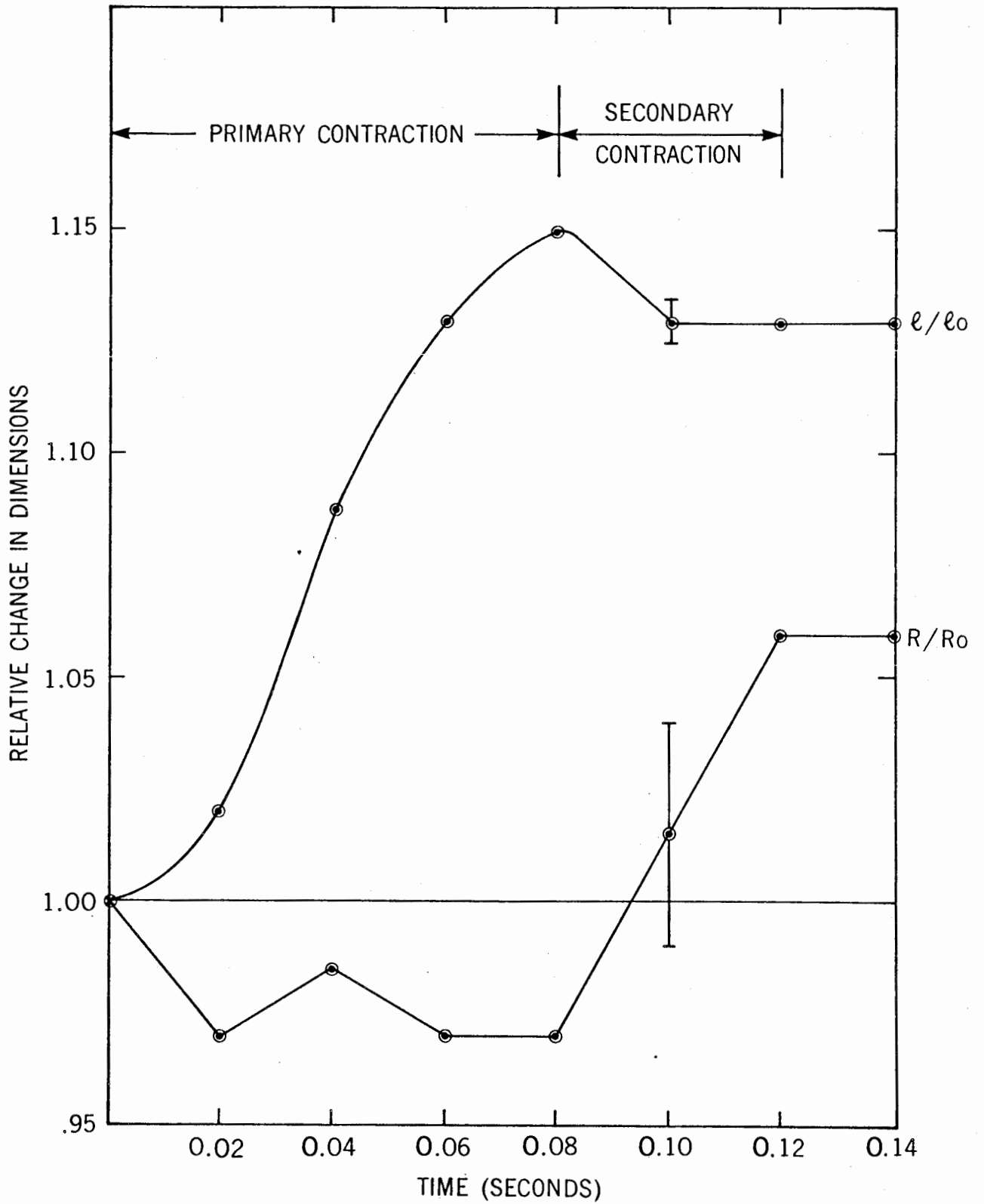
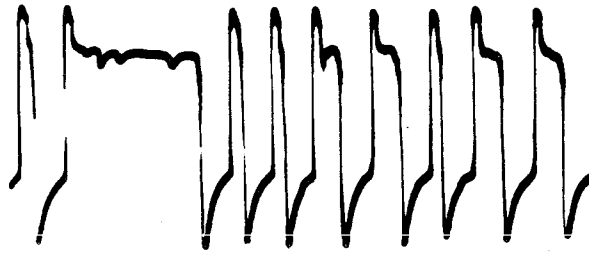


Fig. 3-5

Pharynx muscle action potentials recorded internally from the posterior region of the pharynx during repetitive activity.

- A. The membrane depolarizing at regular intervals and showing plateaus of varying intervals.
- B. Another example showing longer plateau with a slow exponential return towards the resting potential. The slow repolarization ended with a rapid hyperpolarization as in the normal action potential.



20mV  
1sec

A



10mV  
1sec

B

C. Propagation Velocity of the Electrical Activity in the Isolated Pharynx

Radial muscle contraction is initiated by a depolarization of the pharynx membrane and muscle relaxation is initiated by a repolarization of the membrane (Fig. 3-5A). The conduction velocity of the depolarization and repolarization phases of the pharynx membrane action potential were studied by the following experiment.

1. Methods

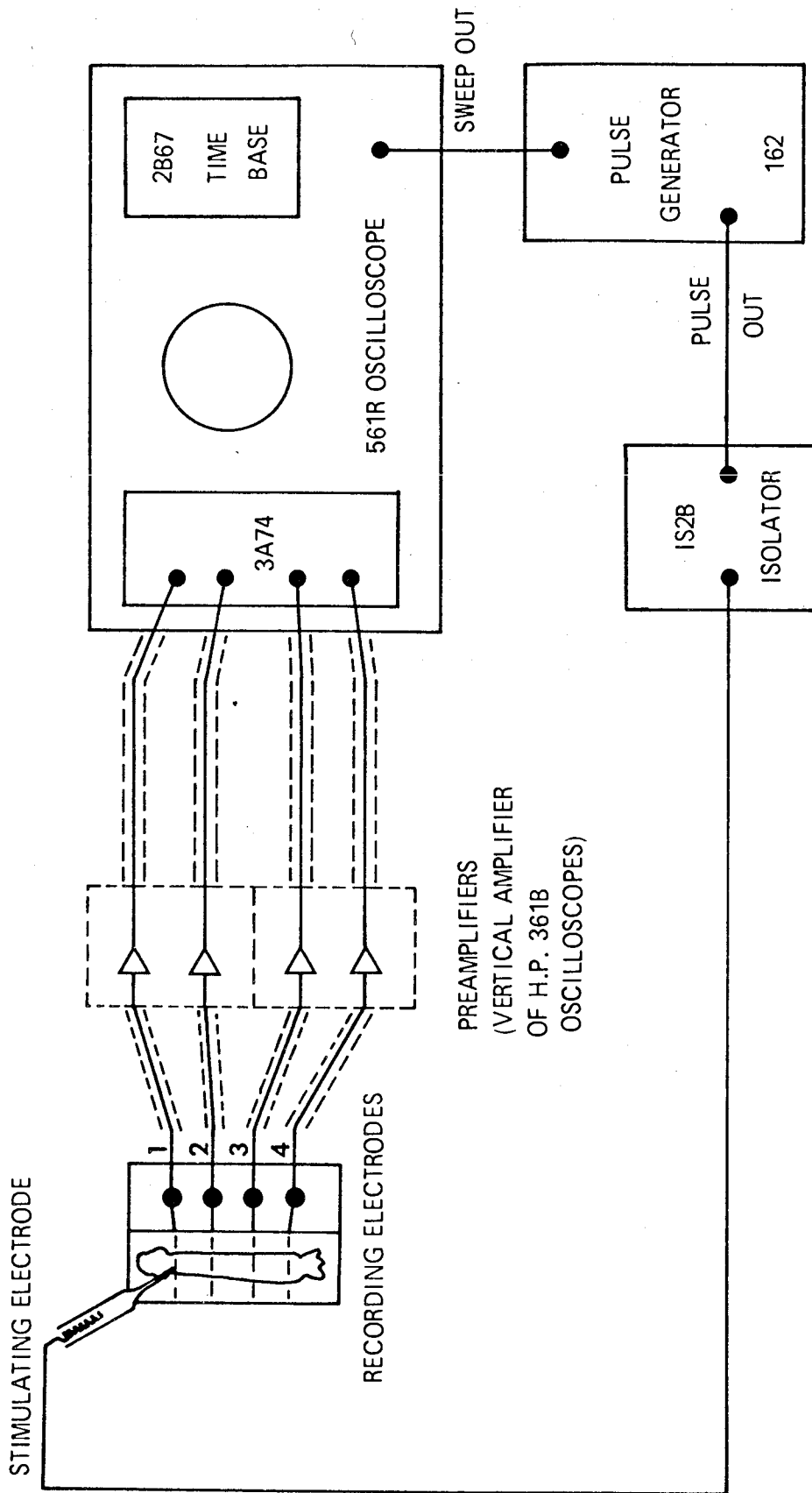
It was impractical to monitor the simultaneous electrical events with two internal electrodes because the electrodes were dislodged when the pharynx lengthened. Flexible external electrodes made of long strands of silver were not very successful because the pharynx had to be lifted from the temperature bath to enable the electrodes to move with the pharynx. When this was done, surface tension distorted the pharynx, and the temperature could not be regulated without resorting to a constant temperature oven.

The experiment was completed successfully with the apparatus shown in Fig. 3-6. The fixed external electrodes, consisting of four .005 inch silver wires, were embedded in plexiglass and exposed only for .5 mm in the bottom of a trough (Fig. 2-2). The muscle was held down gently against the electrodes by surface tension. The electrode apparatus was placed in the constant temperature chamber (Fig. 2-1) and maintained at 37°C.

Fig. 3-6

Circuit block diagram of the apparatus used to measure the velocity of propagation of the action potential.





PREAMPLIFIERS  
(VERTICAL AMPLIFIER  
OF H.P. 361B  
OSCILLOSCOPES)

The signals detected by the external electrodes were set up by ionic currents flowing through the membrane and were thus approximately the differential of the action potential (Fig. 3-7). Three or four channels of information were fed through preamplifiers to the input of a Tektronix 3A74 four channel vertical amplifier on a Tektronix 561R oscilloscope. Oscilloscope traces of the electrical activity due to spontaneous or stimulated contraction versus time were recorded on Polaroid film. Stimulating pulses were applied through a Bioelectric Instruments IS2B isolator and a separate glass microelectrode to all preparations not contracting spontaneously within 5 minutes. The Tektronix 162 pulse generator was triggered by the oscilloscope sweep voltage (Fig. 3-6).

The film was analyzed with a travelling microscope. The position of the depolarization phase and repolarization phase of the action potential at each electrode were recorded. The difference between these positions,  $\Delta d$ , was used to calculate the conduction velocity.

## 2. Results and Discussion

The velocities of the depolarization and repolarization were calculated using the following relationship:

$$\bar{v} = \frac{\Delta s}{\Delta t} = \frac{\Delta s}{\frac{c_o}{c_p} \Delta d} \quad (\text{Equation 3-2})$$

where

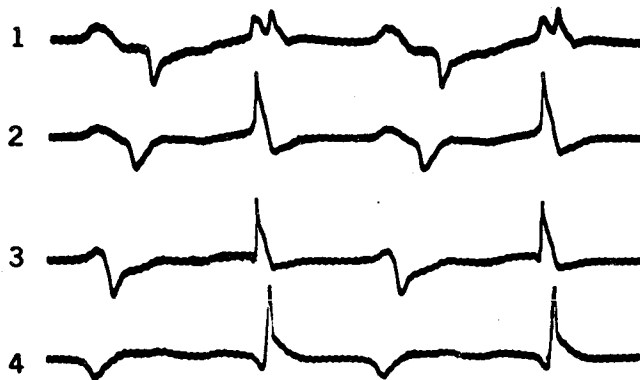
$\Delta s$  - the average electrode separation =  $0.196 \pm .006$  cm

Fig. 3-7A


Spontaneous electrical activity recorded with 4 external electrodes from an isolated pharynx. Electrode 1 is at the anterior end and electrodes 2-4 are spaced posteriorly 0.20 mm apart. The differential of two action potential sequences were observed, each initiated by depolarization (rounded negative deflection) and terminated by repolarization (sharp positive spike). In both sequences, the depolarization originated in the region of electrode 4 and spread anteriorly whereas the repolarization originated between electrodes 2 and 3 and spread anteriorly and posteriorly. Note that the action potential duration was greatest in the region of the original depolarization (electrode 4).

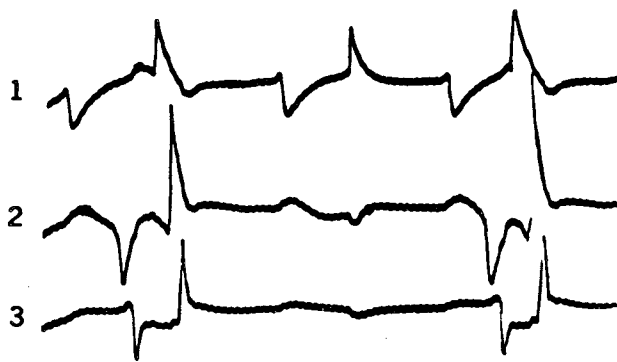
Fig. 3-7B

Three sequences illustrating the case where both depolarization and repolarization originate in the region of electrode 1. Note the absence of membrane propagated electrical activity at electrodes 2 and 3 in the second sequence.



A

2mV   
0.2sec



B

$c_p$  - photograph calibration =  $0.965 \pm .003$  cm/division

$c_o$  - oscilloscope calibration =  $0.20$  sec/division

$\overline{\Delta d}$  - average measured distance between events on the photographs.

The data were grouped, first to determine the difference, if any, in the depolarization and repolarization velocities, and second to determine whether these velocities depended on position along the pharynx. Statistical analysis was used to overcome the problem of variability when interpreting the data.

a) Differences in depolarization and repolarization velocities.

Photographs were chosen in which both depolarization and repolarization data were recorded. One set of data per photograph and two sets per pharynx preparation (on the average) were selected for analysis. Using equation 3-2, the mean velocity of depolarization ( $\overline{v}_c$ ) was calculated to be  $4.0 \pm .20$  cm/sec from 35 determinations of  $\Delta d$ , whereas the mean velocity of repolarization ( $\overline{v}_R$ ) in the same preparations was calculated to be  $5.8 \pm .23$  cm per sec. The uncertainties shown are standard errors.

As  $\overline{v}_c$  and  $\overline{v}_R$  are statistically determined values, the difference shown could occur by chance. Application of Student's t-test predicts that the probability of a chance difference of this magnitude is less than .001.

The significance of the  $\overline{v}_R$  being greater than  $\overline{v}_c$  is that action potential duration is not a constant. The duration will be greatest at the pacemaker site and will be progressively less along the pharynx because the repolarization phase tends to "catch-up" to the depolarization phase. This important finding will be incorporated into the mathematical model of the pharynx.

b) Velocity as a function of position along pharynx.

Photographs were chosen such that data from adjacent electrodes along the pharynx could be determined for both the depolarization phase and/or repolarization phase.

The mean velocity of depolarization toward the anterior or posterior region of the pharynx using these data (18 measurements) were both 3.8 cm/sec.

Towards the anterior the mean velocity of repolarization ( $\bar{v}_{RA}$ ) was  $5.0 \pm .37$  cm/sec whereas towards the posterior the mean velocity of repolarization ( $\bar{v}_{RP}$ ) was  $6.3 \pm .32$  cm/sec (standard error, 15 measurements). The probability of this difference occurring by chance was less than 0.02 as calculated by Student's t-test.

c) Factors contributing to the variation in velocity.

Besides small random variations in velocity due to temperature change and variation in physiological state, three things contribute to velocity variability.

i) Movement error. Relative to the external electrodes, the pharynx was only fixed at one point (alternately anterior and posterior). Therefore, the velocity of action potentials propagated away from the fixed point were too large because of pharynx movement caused by muscle contraction. The true action potential velocity was recorded, however, if the direction of action potential propagation was towards the fixed point. The magnitude of the movement error depends on the speed of muscle contraction. On the average the error in the average velocity would be less than 7.5%, or one half the average elongation of the pharynx.

ii) Spontaneous activity. Spontaneous activity introduced an error in the measurement of velocity because the pacemaker, although apparently stationary in a given preparation was observed to be at different positions in different preparations. In addition, depolarization and repolarization could originate at separate pacemaker sites. The position of the active site introduced an error when the activity originated between two electrodes, because the electrical activity spreads in both directions. The velocity as measured by electrodes adjacent to a pacemaker region would therefore be too large. This error is impossible to detect unless the time of arrival at the two electrodes is simultaneous, or the active region is between the center two electrodes of the four-electrode system (Fig. 3-7A, traces 2 & 3).

iii) Junctions within pharynx. Previous workers, (del Castillo and Morales, 1967a) have reported that there was no barrier to the spread of electrical activity along the pharynx of Ascaris. In fact, they found it convenient to consider the pharynx as a single giant cell. Fig. 3-7B illustrates clearly that this is not true. The first action potential sequence illustrates normal spontaneous activity originating at the anterior region, with conduction posteriorly. There appears to be considerable delay between electrodes 1 and 2, and less delay between electrodes 2 and 3. The second action potential sequence is not propagated, however, and electrodes 2 and 3 show only electrotonic activity due to electrical activity in the region of electrode 1. Thus

the conduction of the electrical activity failed, possibly owing to a junction between cells within the pharynx. A variable junction effect is a possible cause of the observed variability of the normal depolarization and, possibly, repolarization velocities. It could also introduce a delay, lowering the measured values of depolarization and repolarization velocities.

The movement artifact and spontaneous activity errors, on the average, should affect depolarization and repolarization velocities an equal amount. The errors are random events, unrelated to physiology. However, the junction effect could be more important in the determination of  $\bar{v}_C$  and  $\bar{v}_R$  if the junction had rectifier properties, delaying the propagation of depolarization more than repolarization.

d) Some observations on the electrophysiology of the pharynx membrane.

Fig. 3-5A illustrates repetitive pumping just as the pharynx starts to "stick" in the contracted state (showing plateaus of varying duration). Whereas Fig. 3-5B, a different preparation, shows a long duration plateau, with an exponential decay or repolarization. Both oscilloscope traces show the spontaneous subthreshold (SST) activity observed for this membrane. Fig. 3-5A shows repolarizing SST potentials observed in the depolarized state. Fig. 3-5B shows the depolarizing SST activity in polarized state, and very small SST repolarization potentials in the depolarized state.



#### D. Pressure Changes Within the Isolated Pharynx During Pumping

##### 1. Method

Myofilament force and pressure changes within the pharynx were monitored externally with an indentation pressure gauge, Fig. 3-8. An indentation was made in the pharynx with a 000-insect pin. The indentation depth, with the pharynx at rest, is a function of the elastic properties of the membrane and the pressure within the pharynx (Harris and Crofton, 1957). During a pumping sequence, the indentation is pulled in (increased) by myofilament force and pushed out (decreased) by pharyngeal pressure. Therefore, deflection of the insect pin is an indirect measure of the difference between pressure increase and myofilament force per unit area at the outer membrane of the pharynx. Pressure increase is the larger of these values, thus the indentation decreases over-all on myofilament contraction.

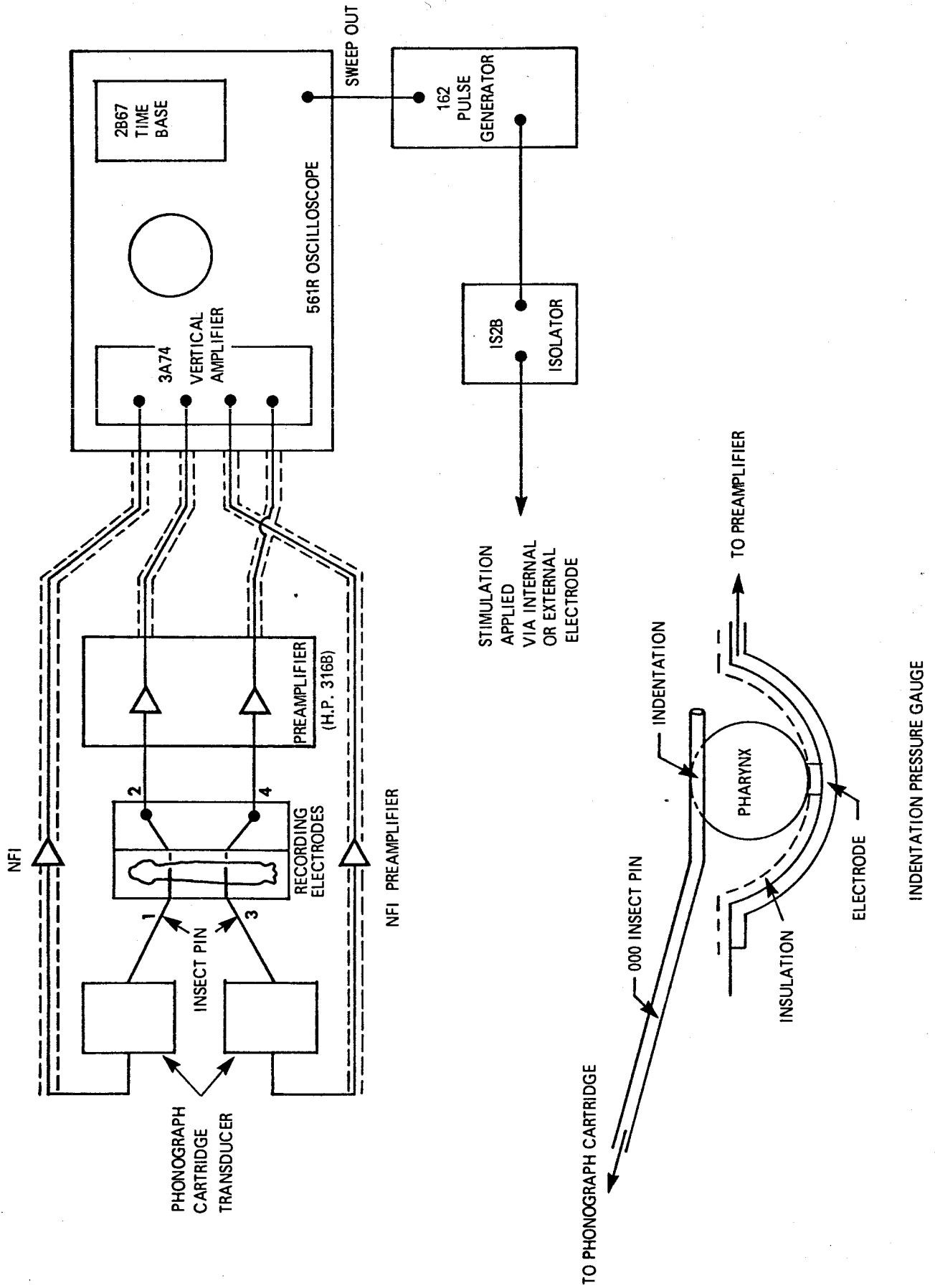
The deflection of the pin was monitored with a ceramic phonograph cartridge and displayed on the oscilloscope screen simultaneously with the electrical events at that point on the pharynx (Fig. 3-8). Two such pressure gauges and associated electrical contacts were used to detect pressure changes along the pharynx as the action potential spread down the organ.

##### 2. Results and Discussion

Fig. 3-9A shows the relationship between electrical activity and pressure changes within the pharynx as monitored with the indentation pressure gauge. There is an approximate 20 msec delay between the

Fig. 3-8

Circuit block diagram of the apparatus used to detect electrical activity and pharynx pressure changes during muscle contraction.



INDENTATION PRESSURE GAUGE

Fig. 3-9A            Pharynx electrical activity (trace 1) recorded simultaneously with pharynx pressure by an indentation pressure gauge (trace 2).

Fig. 3-9B            Simultaneous recording of pressure and electrical events at two points 0.4 mm apart.

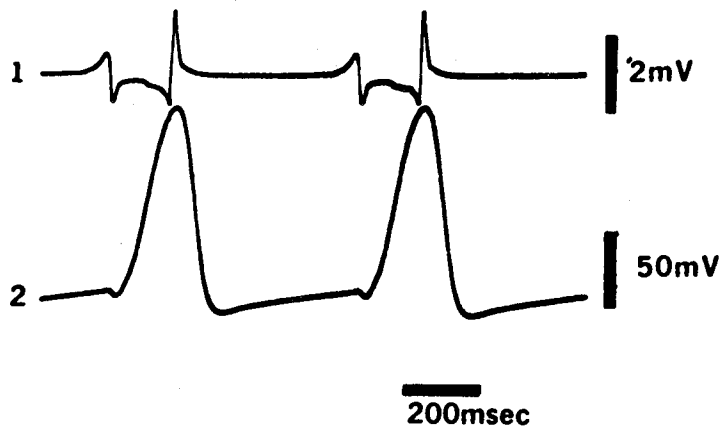
Trace 1 - anterior pressure changes

Trace 2 - anterior electrical activity and stimulus artifact

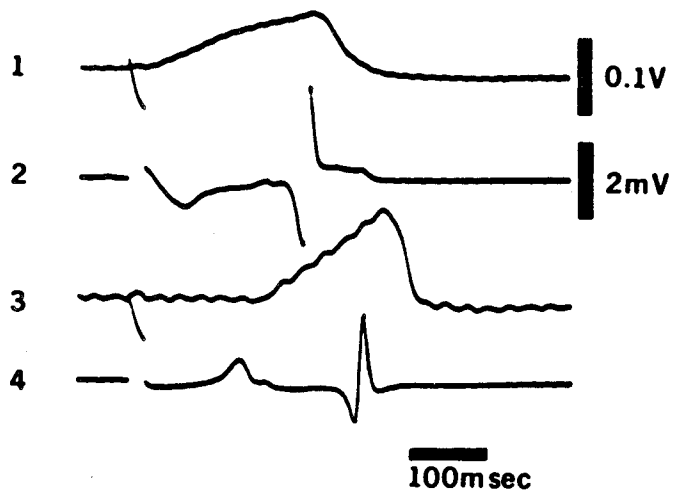
Trace 3 - posterior pressure changes

Trace 4 - posterior electrical activity and stimulus artifact.

Note that there are no pressure changes at trace 3 until depolarization is initiated at this site, the positive deflection shown on trace 4.



A



B

initiation of membrane depolarization and the onset of pressure increase. With the membrane depolarized, the pharyngeal pressure increases rapidly and approaches a maximum. Membrane repolarization initiates muscle relaxation and a rapid decrease in pharynx pressure.

The apparent pressure decrease at the initiation of contraction could be caused by a momentary unbalance of forces at the outer membrane during the period of isometric muscle contraction - that is, before the lumen opens.

Simultaneous recordings of pressure and electrical events at two points on the pharynx are shown in Fig. 3-9B. It was obvious for all traces recorded that depolarization and thus a muscle contraction in one region of the pharynx caused only a localized pressure increase. No pressure increase or decrease was detected at the posterior transducer until pressure changes were initiated by depolarization or repolarization, respectively, at that point. This does not imply that there can be no equalization of pressure within the pharynx. It does mean, however, that such pressure equalizations proceed slowly, more slowly than the conduction of the action potential along the pharynx membrane. Therefore, on the time scale of repetitive pumping, one can consider the pressure changes to be localized at the region of myofilament shortening.

In the reconstruction of the pumping sequence (section F below), it was necessary to know the velocity at which muscle contraction and muscle relaxation moved along the pharynx. The constancy of the delay between electrical and pressure events (Fig. 3-9B) indicated that the values

$\bar{v}_C$  and  $\bar{v}_R$  determined earlier were reasonable estimates of muscle contraction and relaxation phase velocities, respectively.

E. In vivo Pumping Parameters - Summary of Work Done by C. Mapes

Mapes (1966) measured the in vivo pumping rates and pumping capacity of Ascaris by observing the actual transfer of seawater from a chamber into Ascaris intestine. The level of the fluid in a glass capillary was recorded at 64 frames/sec on 16 mm film. The maximum mean pumping capacity determined by this method was  $.33 \text{ mm}^3/\text{pump}$  at a normal rate of 4 pumps/sec ( $1.33 \text{ mm}^3/\text{sec}$ ). The values quoted are for fresh nematodes pumping in short bursts; the pumping rate was observed to decrease slowly with time after removal from the host. In addition, the pumping capacity was much lower, down to  $.05 \text{ mm}^3/\text{sec}$ , in animals pumping over an extended period of time.

In contrast to Mapes' findings, my observations on fresh isolated preparations were a maximum pumping rate of 2.5 pumps/sec and a normal pumping rate of 2 pumps/sec. The pumping rate decreased with time in isolated preparations primarily because of the plateaus of varying duration (Fig. 3-5). In addition, the isolated preparation was seldom observed to pump fluid, indicating that the pumping rate (or possibly damage caused by dissection) was important to the operation of the pharynx as a pump.

#### F. Reconstruction of the Pumping Sequence

The best method of determining the pumping sequence would be to photograph the sequence directly. This could be done with x-rays, if the nematode were feeding on a barium sulfate solution. The experiment was attempted but failed, because the only x-ray cinematography unit available in Vancouver did not have sufficient resolution. Therefore, the sequence was reconstructed on the basis of the results of the experiments described above.

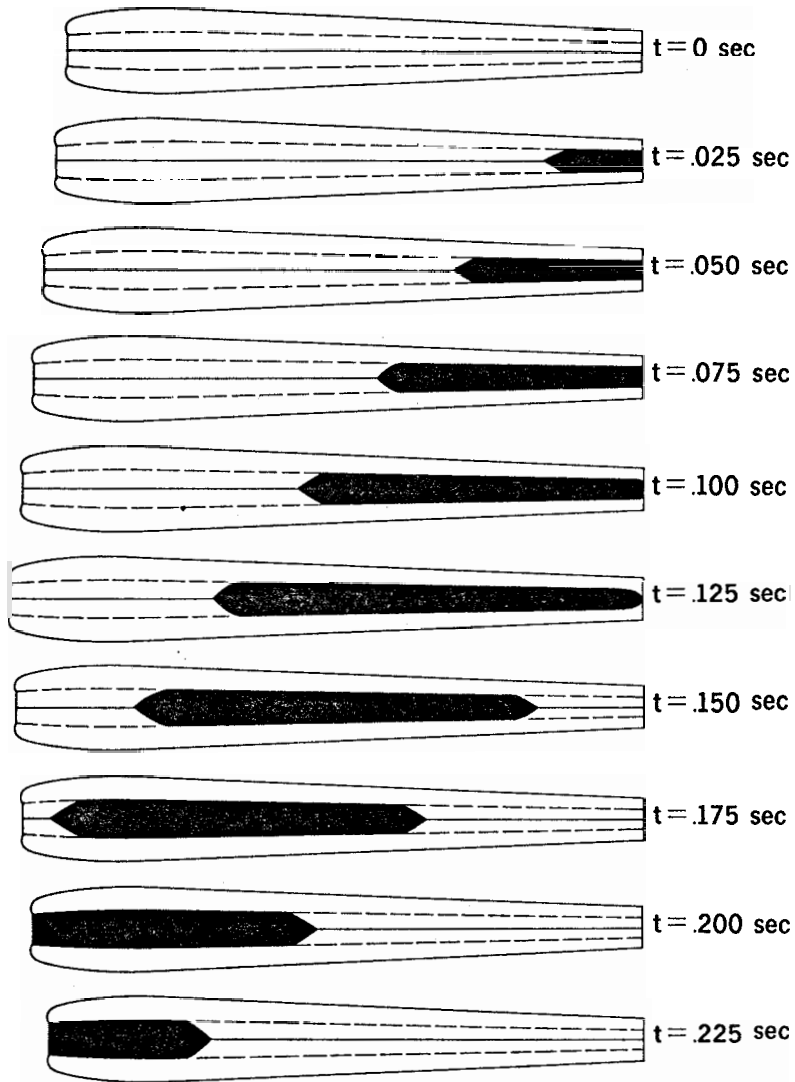
The reconstruction of the pumping sequence is shown in Fig. 3-10. The motion of the lumen must be peristaltic if the pharynx is to pump without regurgitation. Peristaltic motion in the pharynx was described by Doncaster (1962) and in Ascaris was first suggested by Mapes (1965). Mapes speculated that during the ingestion phase of pumping, the lumen would open to the full circle configuration for one half of the pharynx length (his preferred choice) or would open one half the cross-sectional area for the full length. In fact, my results indicate that the lumen opens to almost the triangular configuration (70% of full opening) for approximately 70% of the lumen length. Mapes (1966) also speculated, incorrectly, that the change in external dimensions would be purely radial; my motion picture measurements show the change to be primarily longitudinal.

Contraction (lumen opening) is presumably initiated near the anterior end of the pharynx either by myogenic activity or by enteric nervous system activity, however, the exact location of the pacemaker region is



Fig. 3-10

Diagram of the proposed pumping sequence showing the position of the lumen contents as a function of time.



not known in vivo. In the reconstruction, the pacemaker was considered to be at the anterior tip of the pharynx. Depolarization and hence contraction proceeds posteriorly at an average constant speed of 4.0 cm/sec. Myofilament shortening causes a localized pressure increase within the pharynx muscle which in turn causes a localized lumen opening and a localized extension of the pharynx. This mechanism will be discussed further in Chapter 4.

In vivo, relaxation is initiated approximately 125 msec after the initiation of contraction (Mapes, 1966). In the isolated pharynx, as was shown in this study, the repolarization and hence muscle relaxation proceeds posteriorly at 5.8 cm/sec. Using these figures I estimate that approximately 70% of the lumen length is dilated at the initiation of relaxation, but because  $\bar{v}_R$  is 45% greater than  $\bar{v}_c$ , approximately 50% of the lumen length is closed at the anterior end by the time the contraction phase reaches the end of the pharynx.

After 250 msec, in vivo, a second pumping sequence is initiated at the anterior pacemaker region just as the pharyngo-intestinal valve is closed. The cycle is repeated.

#### G. Forces Acting on the Lumen Contents

The higher value of  $\bar{v}_R$  in comparison to  $\bar{v}_c$ , at first glance would imply that the lumen contents are moved posteriorly by positive lumen pressure at the anterior end. To test this hypothesis, the potential lumen volume gain caused by muscle contraction and potential lumen volume

loss caused by muscle relaxation were calculated.

Let:

$\Delta V_g$  = volume gained in time interval,  $\Delta t$

$r_c$  = the radius of lumen at the point of active  
muscle contraction

$v_c$  = the velocity of contraction phase

Therefore in time,  $\Delta t$ , assuming a circular cross section for the open lumen (see page 68)

$$\Delta V_g = \pi r_c^2 \cdot v_c \cdot \Delta t$$

Also let,

$\Delta V_\ell$  = volume lost due to muscle relaxation in time,  $\Delta t$

$r_R$  = the radius of lumen at the point of active muscle  
relaxation

$v_R$  = the velocity of the relaxation phase

Therefore:

$$\Delta V_\ell = \pi r_R^2 \cdot v_R \cdot \Delta t$$

Assuming the lumen is open for one half of its initial length, the case 0.175 msec after initiation of the pumping sequence (Fig. 3-10), then

$$r_c = 1.5 r_R$$

because the lumen taper is 2:1 for the full lumen length. Thus, the ratio

$$\frac{\Delta V_g}{\Delta V_l} = \left( \frac{1.5 r_R}{r_R} \right)^2 \cdot \left( \frac{4.0 \text{ cm/sec}}{5.8 \text{ cm/sec}} \right) = 1.6$$

A volume ratio this much greater than one is unrealistic for two reasons:

1. Liquids can withstand very large negative pressures without expanding or rarifying, therefore the volume of the lumen contents cannot change once the lumen starts closing.

2. The calculation is based on the assumption that the pharyngeal lumen, at all points along its length is open to the same degree (open to the same cross-sectional configuration). The evidence presented earlier on length changes during a pumping sequence does not support this. In fact, the length change at the posterior of the pharynx is considerably less than the length change at the anterior of the pharynx (Fig. 3-3), suggesting that  $\Delta V_g/\Delta V_l$  is only slightly greater than one.

However, in the tapered region of the pharynx, the lumen volume gained by muscle contraction is potentially greater than the lumen volume lost by muscle relaxation. This is in contradiction to the original hypothesis of positive lumen pressure and it must be concluded that the lumen pressure is negative for a short time after the anterior end of the lumen closes. Therefore, the lumen contents are moved posteriorly by negative pressure. This is supported by Mapes' observation of little regurgitation from the lumen of Ascaris during feeding (Mapes, 1966).

The configuration for volume lost and gained reverses once the contraction phase reaches the end of the tapered region of the pharynx. When this happens, the rapidly advancing relaxation phase pressurizes the lumen contents. When the lumen pressure exceeds the pressure of the pseudocoelom, the lumen contents are injected into the gut.

#### H. Discussion and Conclusion

Reflection on the scheme as proposed leads immediately to the conclusion that the operation of the pharynx is critically dependent on the interrelationship between action potential velocity and action potential duration. Should the velocity be too small or duration too short, the pharynx would operate at low capacity. That is, a small volume would be ingested per pump. If the velocity is too large or the duration too long, there is a distinct possibility that the whole lumen would open at once. Should the pharyngo-intestinal valve open, the intestinal contents (and the intestine) would be regurgitated by the pseudocoelom pressure.

What happens as the nematode grows in size? How are velocity and duration coordinated? There are two possibilities: One, the action potential duration at the pacemaker site could be varied, but there is no evidence at present to support this. Two, a change in action potential velocity ( $v_R$  and  $v_C$ ) proportional to diameter could maintain pumping efficiency as pharynx size changes.

The second possibility has some support for it was found in this study that  $v_R$  (but not  $v_c$ ) increased with position along the pharynx. That is  $v_R$  increased with pharynx diameter. For this reason, the experiment on the velocity of the action potential bears further experimental investigation. It is possible that one of the errors mentioned earlier (page 44) specifically the junction effect, may have masked a functional relationship between  $v_c$  and pharynx diameter.

What is the origin of the increase in  $v_R$  over  $v_c$ ?

1) Stretching of the outer membrane during contraction could increase  $v_R$ . Rapoport (1971), reported that the velocity of the action potential of frog muscle increased by approximately 13% when the muscle was stretched 40%.

2) The shape of the action potential should also contribute to a larger  $v_R$ . The maximum rise time of the action potential is approximately 9V/sec at 39°C, whereas, repolarization takes place at a faster rate and overshoots (hyperpolarizes) 17 mv (del Castillo and Morales, 1967a). Thus one would expect a larger relaxation velocity because the membrane capacitance can be recharged in a shorter time interval.

What is the role of the enteric nervous system? Several possibilities exist:

1. The pharynx is under direct control of the central nervous system (nerve ring) and there is a one to one correspondence between nerve ring activity and pharynx action potentials.

2. The pharyngeal membrane is myogenic (spontaneously active), and pumping activity is controlled via the nervous system by regulating the pharyngeal membrane potential. This control possibility is exactly analogous to the scheme shown to exist for Ascaris somatic muscle by del Castillo, de Mello, and Morales (1963), where acetylcholine acts as a neurohormone regulating the membrane potential.

3. The enteric nervous system is spontaneously active and is somehow controlled by the nervous system external to the pharynx.

Proposal two seems to be the most likely prospect because the isolated pharynx was spontaneously active, but careful experiment will have to be done to prove this. I attempted to reproduce del Castillo's experiments using the pharynx membrane rather than a strip of somatic muscle, but the results were inconclusive. The pharynx pumped repetitively in solutions of piperazine citrate, d-tubocurarine and acetylcholine. In Ascaris somatic muscle, acetylcholine depolarizes the muscle membrane, piperazine hyperpolarizes the muscle membrane and d-tubocurarine blocks the acetylcholine response. These chemicals, applied external to the isolated pharynx were apparently not reaching the active sites on the outer membrane, if in fact these chemicals are active substances for this organ.

Is the pharynx myoepithelium a syncytium? Earlier workers (Goldschmidt, 1905 and Hsü, 1929) have considered the pharynx myoepithelium to be syncytial. This was partially confirmed by Reger (1966) in an electron microscope study of Ascaris pharynx. In examining several hundred sections, he was unable to observe a continuous plasma membrane bounding a single



nucleus. These observations do not answer the question posed, however, because serial sections were not taken through the entire pharynx.

Reger (1966) also reported several types of membrane-membrane appositions, among them an intermembrane contact similar to the "tight junctions" in smooth muscle. He suggested that this junction may function as an electrotonic transmitting synapse. But, if the action potential can be blocked, as was shown in this study, the pharynx muscle cannot be a complete syncytium in Ascaris. Bird (1971) suggested that, because a cellular pharynx has been shown for some nematodes, cellular pharynges may be numerous when serial sections are examined at high resolution.

What is the role of the enteric nervous system and intermembrane contacts in nematode feeding? The viscosity of the small intestine contents could vary considerably; as well as the size, amount and distribution of particulate matter. Therefore, it would be advantageous for the animal to have some control over the pharynx operation (pumping rate, action potential velocity, action potential origin, etc.) in view of the varied properties of the food. For example, decreased pumping rate and lower action potential velocity would be more efficient if the food is very viscous. The question cannot be answered until more work is done in vivo.

This chapter has described the reconstruction of the pumping sequence of the pharynx of Ascaris, based on mechanical, pressure, and electrical observations. Assuming the in vivo pumping rate and using mean experimental action potential velocities as measured on the isolated pharynx, a physically realistic mode of operation for the pharynx of Ascaris was determined.

## CHAPTER 4

### THE MODEL PHARYNX

The physical changes taking place in the pharynx during pumping are too complex for direct analytical computation or intuitive recognition. For this reason, it was decided to extend the pharynx pumping sequence reconstruction of Chapter 3, into a more sophisticated mathematical model of the pharynx. The model approach to the study of the pharynx permitted prediction of the interrelationships between muscle force, pressure, elastic properties, and changing pharynx dimension. The dimensional changes of the model were then checked against changes in the diameter and length of the pharynx as observed through motion picture studies of the pumping sequence.

This chapter is divided into three parts. Part A describes an experiment conducted to determine the static stress-strain relationships in the pharynx membrane. This was necessary because the main analysis in the model is based on pressure induced changes in the external dimensions of the pharynx caused by muscle contraction. Part B of this chapter describes the analysis of the model. Part C discusses the relationships between size, shape, and the efficiency of pumping for the Ascaris pharynx.

#### A. Changes in Dimensions Induced by Osmotic Stress

##### 1. Method

The pharynx was dissected free of the worm as described in Chapter 2. It was placed on a black paraffin block and maintained either at room temperature or at 37°C. A glass coverslip resting on supports

was placed over the pharynx and APF or sucrose solutions of varying concentrations were introduced under the coverglass.

The initial size, in APF, was recorded photographically, using Ilford HP4 film and a Miranda SLR camera. A sucrose solution of approximately 300 milliosmoles (as measured on a Precision Systems, model 2007 osmometer) was exchanged for APF. After 4 minutes the size of the pharynx was recorded. The procedure was repeated for sucrose solutions of varying concentrations, with a range of 80 milliosmoles to 1000 milliosmoles.

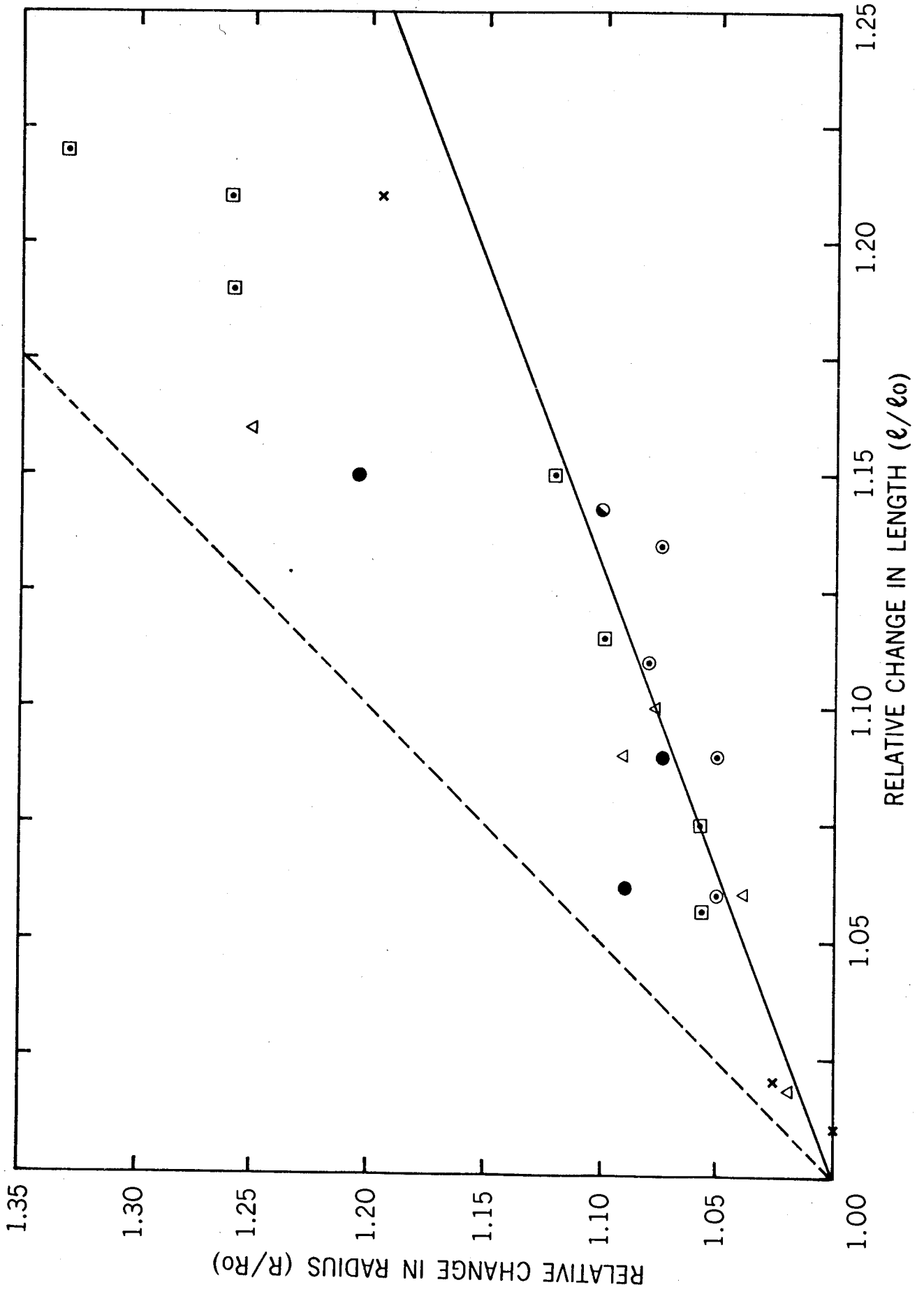
Dimensions were taken from photographic prints using a travelling microscope. The length was determined between convenient anterior and posterior reference points, and the diameter was measured at the widest part of the pharynx.

## 2. Results

The results for osmotic pressure less than 400 milliosmoles are shown in Fig. 4-1. Radial strain ( $R/R_0$ ) is plotted as a function of longitudinal strain ( $\ell/\ell_0$ ). Where  $R_0$ ,  $\ell_0$  are the original radius and length of a segment of pharynx and  $R$ ,  $\ell$  are the radius and length in the same segment under osmotic stress. These results were obtained using six pharynges for increasing and decreasing osmotic stress. The dotted line represents the theoretical curve for a homogeneous Hookian membrane (stress proportional to strain) the same shape as the pharynx. The data indicates that the pharynx membrane is not homogeneous (more easily extended on the long axis) or that there are radial elastic

Fig. 4-1

Relative change in radius ( $R/R_0$ ) as a function of relative change in length ( $l/l_0$ ) for 6 pharynges subjected to osmotically induced pressure stress. The solid line, slope = 0.73, is the average experimental strain-strain curve fitted by regression analysis. The dotted line, slope = 2.0, is the strain-strain curve expected for a homogeneous Hookian membrane.



components in the pharynx; or that both of these alternatives may be present.

The slope of the theoretical curve is 2.0 (see equation 4-17), whereas the slope of the line through the data points between  $\lambda/\lambda_0 = 0$  to  $\lambda/\lambda_0 = 1.15$  is 0.73. These data and the theoretical curve are discussed in the model, the point to be emphasized here is that the pharynx can extend both radially and longitudinally in response to an osmotic pressure induced stress. However, the pharynx does not change its radial dimensions appreciably in response to muscle induced pressure stress during pumping.

### 3. Discussion .

The scatter in the results, Fig. 4-1, for longitudinal strains of 15% or more, were caused by large inelastic stretching of the pharynx membrane. For strains less than 15%, the data are more consistent, but there is still considerable uncertainty. The uncertainty in the data was attributed to the following points:

#### a) longitudinal strain

- i) lack of clear reference markers upon which to set the microscope cross hairs.
- ii) bending of the pharynx along the longitudinal axis due to unequal inelastic stretching of longitudinal components.

#### b) circumferential strain

- i) localized bulging of the pharynx
- ii) small dimensional changes relative to the reading uncertainty of the microscope.

c) general inelastic stretching between longitudinal and radial readings, that is, the strain-strain curve (Fig. 4-1) may not be linear.

Other comments on this data, as it applies to the pharynx, will be made in Part B of this chapter.

## B. The Model Pharynx

### 1. Assumptions and definitions

In constructing a model of the pharynx, the following simplifications were made:

a) the model is considered as two co-axial truncated cones with variable radii. The inner cone radius can reduce to zero to represent the closed lumen. The lumen in vivo is triradiate, and probably never achieves a circular cross sectional configuration during repetitive pumping, but this should not affect the results. It is the volume generated within the lumen, independent of shape, which is the important consideration in this analysis.

b) no body forces are considered, that is, the membranes are weightless relative to the muscle force, pressure, etc.

c) any elastic forces produced by the lumen and marginal tissue are considered to be produced by the external membrane.

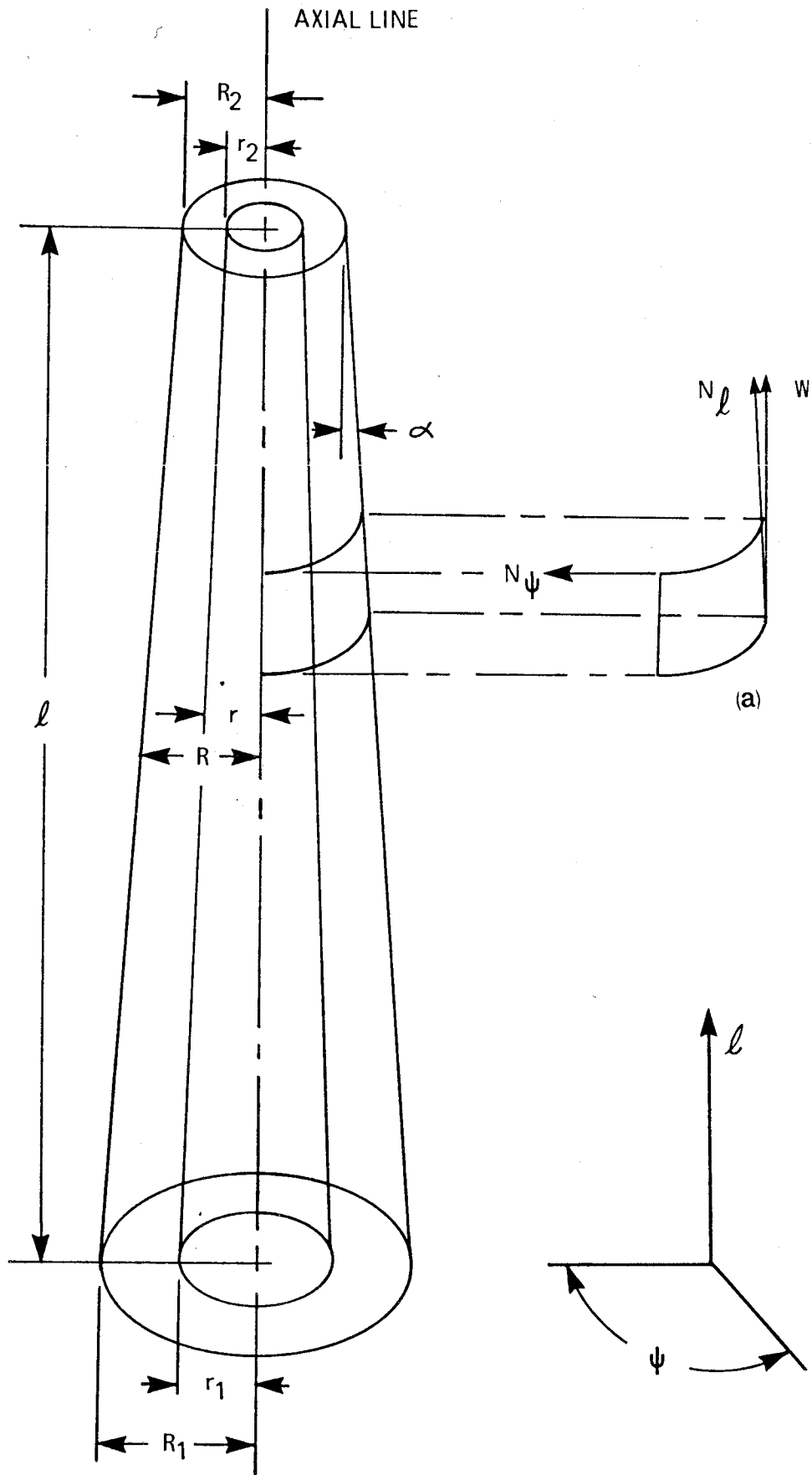
A schematic diagram of the model pharynx is shown in Fig. 4-2. The development of the model is sufficiently general that the length,  $\ell$ , may represent the whole length of the pharynx, or any portion of that length. Thus the local changes in dimensions that were observed can be considered with the same model. In addition,  $r$ ,  $R$ , and  $\ell$  (the general case) are variables during contraction.

Fig. 4-2

Schematic representation of the model pharynx.

The diagram is not to scale as the ratio  $\ell/R_1$  was made small for clarity. The cut-out (a) defines the direction of  $N_\psi$ ,  $N_\ell$  and  $W$ .





To indicate the relative dimensions of the average pharynx and the model, the following ratios and constants are given. If  $\ell$  represents the full length of the pharynx then;

$\ell/2R_1 \approx 5$  is the length to diameter ratio of the tapered region of the pharynx,

$$\frac{r_1}{R_1} = \frac{r_2}{R_2} = 0 \text{ to } 1/2 \text{ during contraction,}$$

$$\frac{R_1}{R_2} = \frac{r_1}{r_2} = \beta = 2 \quad (4-1)$$

and

$\alpha = 5.5^\circ$ , the cone semiangle of the outer cone.

When  $r = 0$ , myofilaments relaxed, let:

$$R_1 = R_{10}, R_2 = R_{20} \text{ and } \ell = \ell_0 \quad (4-2)$$

The radially oriented myofilaments exert a total force  $F$ , a force per unit area  $F_r$  at the lumen surface, and a force per unit area  $F_R$  at the outer surface.

The forces acting on the pharynx outer membrane, are:

$P_p$  = pharynx pressure

$P_b$  = pseudocoelom pressure

$F_R$  = myofilament force per unit area

Pharynx pressure  $P_p$  opposes  $P_b$  and  $F_R$ . There is no evidence of a

rigid structure within the pharynx. Therefore, for equilibrium of forces on the outer membrane,  $P_p$  must always be greater than  $P_b$ . That is, in excess of 70 mm of Hg, the normal pressure in the body cavity (Harris and Crofton, 1957).

In isolated preparations,  $P_p$  is definitely greater than atmospheric pressure because;

a) slight damage to the pharynx causes the contents to ooze out

b) if the damage is extensive, but not sufficient to block muscle contraction completely, the outer surface of the pharynx collapses on myofilament shortening.

If  $P_l$  is the lumen pressure, then

$$P_p > P_b \geq P_l \quad (4-3)$$

is the condition for lumen opening. The condition for lumen closing, at the end of the pumping sequence is:

$$P_p > P_l > P_b \quad (4-4)$$

## 2. Conditions for opening the lumen

The lumen starts to open when the myofilament normal force per unit area  $F_r$  just exceeds the pressure difference  $P_p - P_l$ . As a result of the angle of insertion of the myofilaments, this will occur first at the "V" or mid-point of the triradiate lumen (Fig. 4-3). The opening force will pull the lumen radially at the "V", flexing the lumen. The lumen is flexible as is readily seen in photomicrographs (Fig. 4-5A and del Castillo and Morales, 1969).

Fig. 4-3

Schematic cross sectional view of the nematode pharynx, illustrating in;

segment 1, the triradiate lumen closed

segment 2, the postulated lumen configuration

when pulled open very slowly via myofilament

contraction (myofilaments not illustrated for simplicity)

segment 3, the postulated lumen configuration when

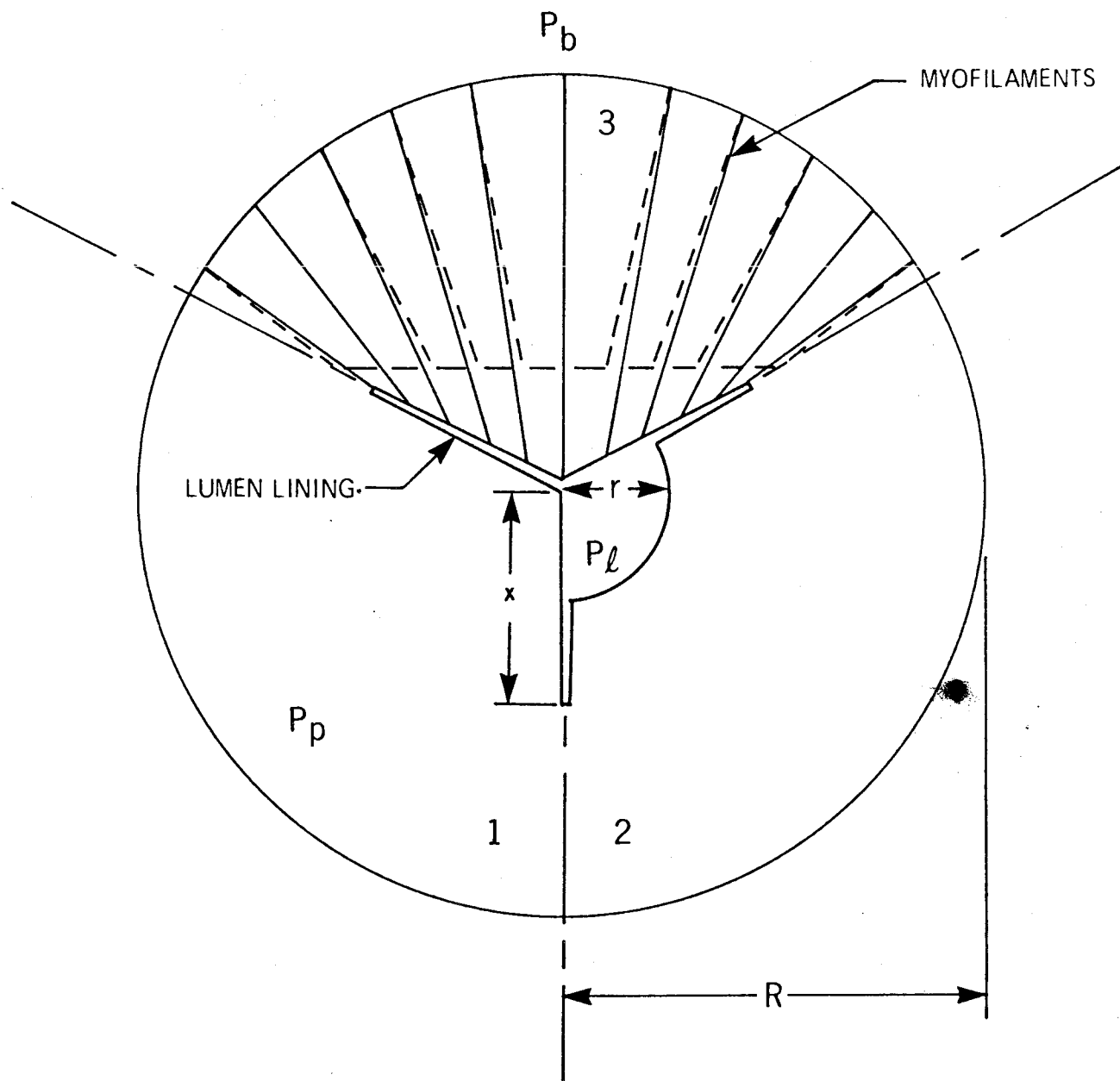
pulled partially open via rapid myofilament

contraction. Two views of the myofilaments are

shown; solid lines represent myofilaments in

relaxed state, dotted lines represent the

myofilaments in a hypothetical contracted state.



The flexing of the lumen changes the angle of nearby myofilaments to near normal, and they may then pull the lumen open further. At first glance, it might appear that opening could then proceed regeneratively until the full open configuration was reached. This does not occur, however, because the opening of the lumen is accomplished only at the expense of an increase in  $P_p$ , and the consequent elastic deformation (elongation) of the pharynx. Thus, for any constant myofilament force less than the maximum force required for full opening, there will be a unique, stable, partially open configuration of the lumen, approximately circular in cross-section, although, exactly how circular will depend on the exact flexibility of the lumen and the myofilament orientation.

The argument presented above is valid only for very slow lumen opening, when the myofilament normal force  $F_r$  just exceeds the equilibrium normal force for that degree of opening. Normally the lumen opens very rapidly during sequential pumping therefore  $F_r$  must greatly exceed  $P_p - P_\ell$  (see page 88).

### 3. Myofilament force per unit area

In a thin cross-sectional slice of pharynx with a thickness  $\Delta\ell$ , the myofilaments exert a total force  $dF$ . At the outer membrane,

$$F_r = \frac{\text{force}}{\text{area}} = \frac{dF}{2\pi R \Delta\ell} \quad (4-5)$$

If the force  $dF$  is just able to maintain the lumen open to a radius  $r$ , then

$$F_r = \frac{dF'}{2\pi r \Delta\ell} \quad (4-6)$$

where  $dF'$  is the normal force exerted by the myofilaments inserted on the open region of the lumen (Fig. 4-3).

The fraction of myofilaments opening the lumen for any radius  $r$ , is  $2\pi r/6x$  where  $x$  is the length of one ray of the triradiate lumen.

Thus

$$dF' = dF \left( \frac{2\pi r}{6x} \right)$$

Therefore, equation 4-6 becomes

$$F_r = \frac{dF}{6x\Delta\ell} \quad (4-7)$$

Combining equations 3-1, 4-5 and 4-7

$$F_r = 2.3 F_R \quad (4-8)$$

The assumptions made in deriving equation 4-8 are:

- a. it is valid only for very slow opening,  $F_r$  just exceeding  $P_p - P_\ell$  (the lumen opening maintains a circular cross section)
- b. the circumferential strain is not large,  $R \approx R_0$  at all times
- c. the angle of myofilament insertion on the open region of the lumen is  $90^\circ$ .

#### 4. The relationship between $R$ , $\ell$ , and $r$

When  $r = 0$ , the volume enclosed by the outer cone representing the model pharynx is

$$V_1 = 1/3\pi R_0^2 \ell_0 \quad (4-9)$$

If  $r = r_1$ , the volume between the cones is

$$V_2 = 1/3\pi R_1^2 \ell - 1/3\pi r_1^2 \ell \quad (4-10)$$

Also,  $V_1 = V_2$  because the pharyngeal contents are incompressible and no cytoplasm is lost during pumping. Therefore, equating 4-9 and 4-10 and simplifying

$$\frac{\ell}{\ell_0} = \frac{R_{10}^2}{R_1^2 - r_1^2} \quad (4-11)$$

Equation 4-11 is plotted in Fig. 4-4. The relative length change ( $\ell/\ell_0$ ) as a function of relative radius change ( $R/R_0$ ) is shown for two values of ( $r/R_0$ ). The values of  $r/R_0$  were chosen for the lumen full open (circular configuration) and for the lumen partially open. The partially open configuration was chosen such that the value of  $r$  resulted in a lumen cross sectional area equivalent to that expected if the lumen had opened to a triangular configuration. The triangular configuration would be obtained if the lumen flexed only at the "V" and apicies as the lumen opened.

##### 5. Normal opening of lumen

As pointed out in Chapter 2, in the isolated pharynx repetitive pumping causes only an approximately 15% length strain  $\left( \frac{\ell - \ell_0}{\ell} \cdot 100\% \right)$  and negligible radial strain. On that basis, Fig. 4-4 indicates that the lumen is not fully open during normal pumping in the isolated pharynx. The dimensional changes are consistent with the lumen opening to the equivalent of the triangular configuration. Therefore, the average maximum volume ingested by the pharynx is predicted to be:

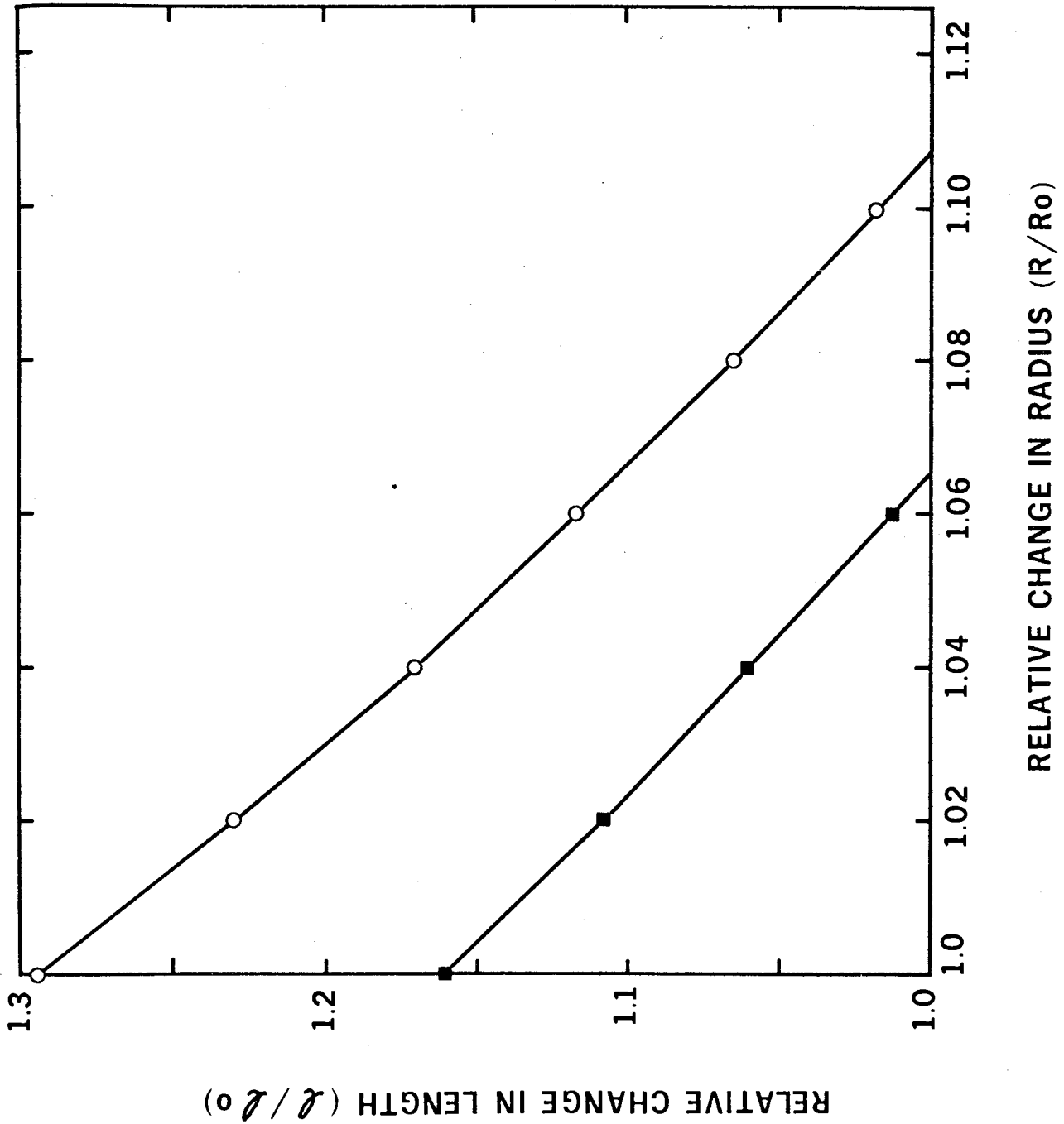


Fig. 4-4

Relative length change as a function of relative radius change for two magnitudes of lumen opening, equation 4-11.

o - lumen full open to the extent allowed by the dimensions of the lumen ( $r=R_o/2$ )

■ - lumen partially open ( $r=.742 \times R_o/2$ ), equivalent to the lumen opening to a triangular cross section.



length of lumen open = 40 mm/sec x .125 sec = 5 mm

area of lumen at widest point = .12 mm<sup>2</sup>

area of lumen at anterior end = .044 mm<sup>2</sup>

volume of open lumen = .39 mm<sup>3</sup>

This value compares favourably with the average maximum volume per pump (.33 mm<sup>3</sup>/pump) calculated from Mapes' (1966) data for in vivo pumping.

The lumen can be opened beyond the triangular configuration if relaxation should fail to occur, that is, if sequential pumping terminates in the membrane depolarized state, a normal occurrence after a period of active pumping. This secondary contraction phase causes primarily a radial increase in the external pharynx dimensions. The data of Fig. 3-4 indicate that for this particular example, radial strain was  $.06 \pm .025$  and longitudinal strain was  $.130 \pm .005$ . Location of the data points (1.06 and 1.13) on Fig. 4-4 suggests that the lumen opened from the triangular configuration to the full open or circular configuration during the secondary contraction phase.

In conclusion, the pharynx lumen can be opened to the full extent allowed by its dimensions. However, during repetitive pumping it normally does not reach this full open state. The relaxation phase is initiated sometime before the muscles reach full contraction.

## 6. The relationship between stress, strain, and myofilament force

### a) Theory and definitions

The analysis of the model necessary to correlate circumferential and longitudinal stress with muscle forces was done using the membrane

theory of shells. The equations are presented here, after all assumptions were considered.

Membrane equations were derived considering the equilibrium of forces for a conical shell. The bending stress resultant is neglected in membrane theory and all other shears or twisting resultant are zero for axial symmetry. In addition, the body forces, weight of membrane, are considered small in comparison to the muscle force. Therefore, from Turner (1965), page 27:

From the conditions of moment balance

$$N_{\psi} = \frac{-PR}{\cos\alpha} \quad (4-12a)$$

From the conditions of horizontal equilibrium

$$N_{\ell} = \frac{W}{\cos\alpha} \quad (4-12b)$$

From the conditions of vertical equilibrium

$$WR = - \int PRdR + V \quad (4-12c)$$

Where,

$N_{\ell}$ , for the cone is a circular line of force (force per unit length) with the force in the direction of the axial line, parallel to the membrane (Fig. 4-2).

$N_{\psi}$ , a line of force, for the cone a straight line, the force vector tangent to the circular cross section of the cone.  $N_{\psi}$  and  $N_{\ell}$  are analogous to surface tension, but are not constants as in a liquid.

P, pressure difference between inside and outside of the membrane, larger inside pressures are considered negative by Turner.

R, radius

W, force per unit length parallel to the axial line (Fig. 4-2).

Equation 4-12b gives the relationship between W and  $N_{\ell}$ .

$\alpha$ , cone semiangle (Fig. 4-2).

V, the applied axial loading constant, the force per unit radian parallel to the axial line.

In addition, let

$\epsilon_{\ell} = \Delta\ell/\ell$ , be the longitudinal strain

$\epsilon_{\psi} = \Delta R/R$ , be the circumferential or radial strain

$\tau$ , the thickness of the membrane

$E_{\psi}$ ,  $E_{\ell}$ , the elastic constants for the membrane in the circumferential and longitudinal directions

$\sigma_{\ell}$ , the longitudinal stress

$\sigma_{\psi}$ , the circumferential stress

Therefore, by definition

$$E_{\psi} = \frac{\sigma_{\psi}}{\epsilon_{\psi}}, \quad E_{\ell} = \frac{\sigma_{\ell}}{\epsilon_{\ell}} \quad (4-13 \text{ a, b})$$

$$N_{\psi} = \frac{\sigma_{\psi}}{\tau}, \quad N_{\ell} = \frac{\sigma_{\ell}}{\tau} \quad (4-14 \text{ a, b})$$

Equations 4-12 a, b, c; 4-13 a, b; and 4-14 a, b; will now be used to test various configurations of the model pharynx via the ratio  $\epsilon_{\psi}/\epsilon_{\ell}$ , the ratio of circumferential strain to longitudinal strain. Note  $\epsilon_{\psi}$  is numerically equal to either  $\Delta D/D$  (diameter) or  $\Delta R/R$  (radius).

b) Simple conical pressure cylinder

Assuming the pharynx is a simple conical pressure cylinder with closed ends constructed of a homogeneous Hookian membrane ( $E_\psi = E_\ell$ ) of uniform thickness, what is the strain/strain ratio?

For constant pressure, equation 4-12c becomes

$$WR = \frac{-PR^2}{2} + V \quad (4-15)$$

At a general point R,

$$2\pi RW = -P\pi R^2$$

hence,  $V = 0$

Therefore, from equations 4-12 a, b and c

$$N_\psi = \frac{-PR}{\cos\alpha}, \quad N_\ell = \frac{-PR}{2\cos\alpha} \quad (4-16 a,b)$$

Dividing

$$\frac{N_\psi}{N_\ell} = 2 \quad (4-17)$$

Also, using equations 4-13 and 4-14,

$$\frac{\epsilon_\psi}{\epsilon_\ell} = 2 \quad (4-18)$$

That is, the relative increase in radius is twice the relative increase in length in response to small pressure induced stress.

Since  $\epsilon_\psi/\epsilon_\ell$  was found to be 0.73 in response to osmotic pressure stress (Fig. 4-1), the pharynx membrane was found to be effectively heterogeneous. Using equations 4-13 and 4-17, the ratio of the elastic

constants was calculated to be:

$$E_{\psi} / E_{\ell} = 2.7 \quad (4-19)$$

c) Model pharynx, very slow opening of lumen

In this calculation the myofilaments are opening the lumen, but the contraction proceeds so slowly that the forces acting can be assumed to be in equilibrium at any instant of time.

From equilibrium of forces at a general point R and r

$$2\pi RW = -(P_p - P_b) \cdot (R^2 - r^2)$$

where  $(P_p - P_b)$  is the pressure difference across the outer membrane and r is the radius of the lumen. Hence, from equation 4-15

$$V = \frac{r^2}{2} (P_p - P_b)$$

and from equation 4-12b and 4-12c

$$N_{\ell} = \frac{P_p - P_b}{\cos\alpha} \cdot \frac{R^2 - r^2}{2R} \quad (4-20)$$

An additional term must be included into the pressure term when determining  $N_{\psi}$ . This is the force per unit area ( $F_R$ ) exerted by the myofilaments. An approximation was made here. The angular difference between pressure and  $F_R$  was neglected. This will introduce an error of approximately  $\cos\alpha$ , (less than 1%) in  $N_{\psi}$ .

Therefore, including  $F_R$  in equation 4-16a, and substituting  $P_p - P_b$  for  $P$ ,

$$N_\psi = \frac{\{(P_p - P_b) - F_R\}R}{\cos\alpha} \quad (4-21)$$

Using equation 4-8 and remembering for very slow opening  $F_r = P_p$  we obtain

$$N_\psi = \frac{(P_p - P_b)R}{\cos\alpha} \cdot \left\{ 1 - 0.44 \left( 1 + \frac{[P_b - P_\ell]}{[P_p - P_b]} \right) \right\} \quad (4-22)$$

Thus, from equations 4-20 and 4-22

$$\frac{N_\psi}{N_\ell} = 2 \cdot \frac{R^2}{R^2 - r^2} \cdot \left\{ 1 - 0.44 \left( 1 + \frac{[P_b - P_\ell]}{[P_p - P_b]} \right) \right\} \quad (4-23)$$

Equation 4-23 has three terms. The constant 2 is the ratio expected for a pressure-stressed, closed-end cone or cylinder. The term in  $r$  and  $R$  is introduced as a result of the lumen opening, the cone not being completely closed at the ends. The value of  $R^2/R^2 - r^2$  is summarized for three values of  $r$  in Table 4-1. The last term of equation 4-23 results from muscle force and pseudocoelom pressure.

If  $P_b = P_\ell$ , as in the isolated pharynx then the last term of equation 4-23 becomes a constant (0.56). Therefore, values of  $N_\psi/N_\ell$  may be calculated for various values of  $r$ . In addition,

$$\frac{\epsilon_\psi}{\epsilon_\ell} = \frac{E_\ell}{E_\psi} \cdot \frac{N_\psi}{N_\ell} \quad (4-24)$$



TABLE 4-1

Value of the strain/strain ratio ( $\epsilon_\psi/\epsilon_\ell$ ) for three different values of lumen radius for very slow opening of the lumen.

radius of lumen (general variable r)	$\frac{R^2}{R^2 - r^2}$	$\frac{N_\psi}{N_\ell}$	$\frac{\epsilon_\psi}{\epsilon_\ell} = \frac{N_\psi}{N_\ell} \cdot \frac{E_\ell}{E_\psi}$
r = 0	1.00	1.12	.41
r = .748 ( $R_0/2$ ) equivalent to triangular configuration	1.14	1.28	.47
r = $R_0/2$ full open	1.33	1.49	.54

where  $E_{\psi}/E_{\ell}$  is given by equation 4-19 from the osmotic pressure experiment. The values of  $N_{\psi}/N_{\ell}$  and  $\epsilon_{\psi}/\epsilon_{\ell}$  are summarized for three values of  $r$  in Table 4-1.

These data show that one would expect to observe an average circumferential strain of approximately one half the longitudinal strain for very slow opening. This was in fact observed. If relaxation should fail to occur, muscle force and pressure come to equilibrium as described previously (Fig. 3-4). In this condition,  $\epsilon_{\psi}/\epsilon_{\ell}$  was calculated to be  $0.46 \pm .1$ , a value in good agreement with the theoretical prediction based on the proposed model.

d) Model pharynx, sequential opening of lumen

Why then is  $\epsilon_{\psi}/\epsilon_{\ell}$  observed to be zero during normal sequential pumping? This can be accounted for by noting that the lumen is opening rapidly, therefore  $F_R$  is much greater than the force required for slow opening. An increase in  $F_R$  prevents radial expansion at the expense of greater longitudinal expansion.

An estimate of  $F_R$ , in terms of the pressures involved, may be obtained by referring to equation 4-20 and 4-21. The absolute value of  $N_{\ell}$  is always greater than zero. Therefore,  $N_{\psi}/N_{\ell}$  and thus  $\epsilon_{\psi}/\epsilon_{\ell}$  are zero only when  $N_{\psi} = 0$ .  $N_{\psi}$  is zero when  $(P_p - P_b) - \bar{F}_R = 0$ , equation 4-21, where  $\bar{F}_R$  is the average force per unit area produced by the myofilaments at the outer surface of the pharynx. The average value must be used here because the dynamic force produced by a muscle depends on its speed of shortening measured in relative length change per time

(Katz, 1939). The speed of shortening will depend on the position of the myofilament. It is greatest at the "V" of the lumen and least towards the apices (Fig. 4-3).

In the isolated pharynx ( $P_b = \text{atmospheric}$ )  $\bar{F}_R \approx P_p$  thus from equation 4-8 one can predict that  $F_r$  exceeds  $P_p$  by approximately 100%.

It was also observed that occasionally the circumferential strain was negative. This is easily explained if the pharynx has lost pressure,  $P_p$  is lower, and the myofilaments are capable of exerting a force  $F_R$  in excess of the increase in  $P_p$ . Thus,  $N_\psi/N_\ell < 0$  and circumferential strain is negative.

What happens in vivo when  $P_p > P_\ell$ ? Referring back to equation 4-23, the term  $(P_b - P_\ell)/(P_p - P_b)$  is always greater than zero. A reasonable estimate of the maximum value would be 0.5, when  $P_b = 70$  mm of Hg and  $P_p = 210$  mm of Hg (Harris and Crofton, 1957), and  $P_\ell$  is atmospheric. Also, negative pressures within the lumen ( $P_\ell$  less than atmospheric) would increase this term slightly. The effect of  $(P_b - P_\ell)/(P_p - P_b)$  would be to decrease  $N_\psi/N_\ell$ , that is, higher pseudocoelom pressure favours longitudinal extension over circumferential extension.

In vivo, an opposing force to that caused by pseudocoelom pressure is the force produced by elastic fibers running between body cavity and pharynx. Extension of the pharynx would stretch these fibers, producing an elastic force limiting longitudinal extension. The magnitude of this force could not be calculated, thus an accurate estimate of  $\epsilon_\psi/\epsilon_\ell$  in vivo cannot be made. It is clear however that elongation will be favored over radial increase.

### C. Size, Shape, and Efficiency

#### 1. Maximum diameter of pharynx

D. R. Roggen, 1970, recently asked the following question: "Is there a maximum size for the nematode pharynx?". He considered only diameter of the pharynx as a function of the diameter of the nematode. The results are reproduced in Fig. 4-5. Roggen plotted the dimensions for a number of worms reported in the literature, and found that for all (except one) the data fell on or below the curve shown. The exception was also accounted for by the special position of the duct glands.

His explanation for the shape of the curve went as follows:

a) the pharynx will be of a size to minimize the energy needed for food intake, therefore the diameter of the lumen tends to increase for two reasons:

i) the suction work done on food intake decreases with increasing lumen diameter

ii) muscular efficiency increases with length of the myofilaments

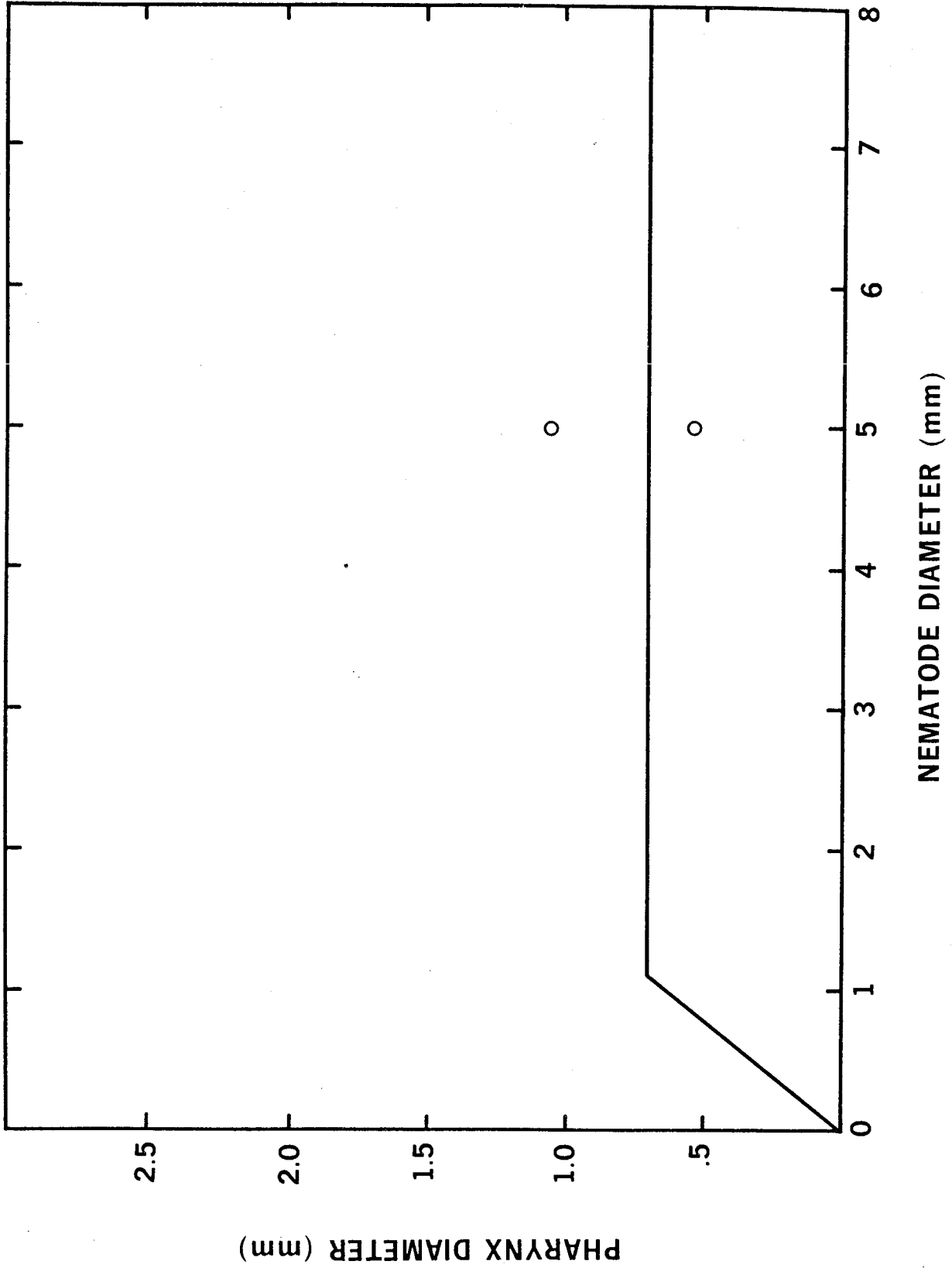
b) the pharynx contains digestive glands and these have to take substrates for enzyme synthesis from the pseudocoelom. There are no known transport systems, therefore diffusion of molecules from the pseudocoelom should impose an upper limit on the pharynx diameter.

#### 2. Limitation to pharynx length

It was not mentioned by Roggen (1970), but the diffusion of high energy molecules to operate the pharynx muscle may also impose an upper limit on the pharynx. With this in mind, I conducted a similar

Fig. 4-5

Diameter of the pharynx as a function of the diameter of the nematode, after D. R. Roggen. Open circles indicate representative dimensions for Ascaris used in this study.



analysis to see if there was a maximum length to the nematode pharynx. The results, representing examples from Strongyles, Ascarids, and some Trichostrongyles, are shown in Fig. 4-6 (Mozgovoi, 1953; Popova, 1958; and Skrjabin, 1954). The ratio of pharynx length to nematode length (the slope of a line between the origin and any point) clearly decreases with increasing nematode length. The ratio is:

- a)  $1/6 - 1/10$  for nematodes of less than 10 mm
- b)  $1/18$  average for nematodes of less than 80 mm
- c)  $1/36 - 1/50$  for nematodes in excess of 200 mm.

Thus, although the results are not as clear cut in this example as in comparison to Roggen's analysis, there is a clear tendency for pharynx length limitation.

The results of Fig. 4-5 and 4-6 demonstrate that the pharynx of Ascaris is limited in volume in comparison to smaller nematodes. Thus, selective pressures may have been present during Ascaris evolution such that the pharynx operate efficiently.

### 3. Efficiency and the elongating pharynx

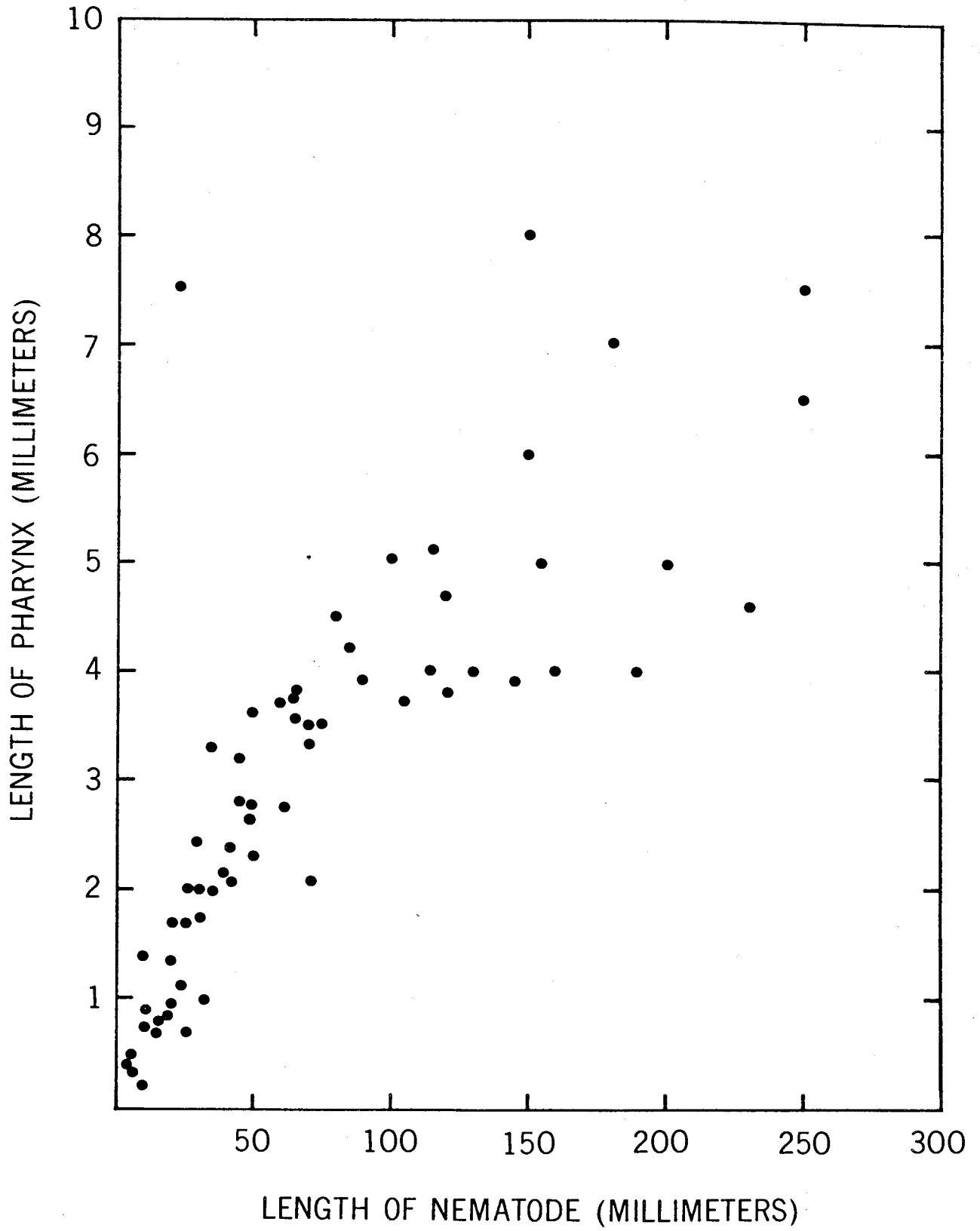
The work done on a fluid is given by the integral  $\int PdV$ .

Therefore, ignoring viscous energy losses, the work done displacing the pseudocoelom contents as the lumen opens is the same for both a longitudinally expanding and a radially expanding pharynx. However, the energy loss terms were not equal for the alternative modes of operation when the viscous loss terms are included. Pseudocoelom fluid displaced at the anterior ends of the pharynx during radial expansion of the pharynx would

Fig. 4-6

The length of the pharynx plotted as a function of the length of the nematode. The results, representing examples from strongyles, ascarids and trichostrongyles, show a reduction in the fraction of the nematode pseudocoelom taken up by the pharynx as nematode size increases.





have to flow through relatively long, narrow and obstructed passages between the pharynx and nematode body wall, whereas the pseudocoelom fluid displaced in the longitudinally increasing pharynx occurs at the posterior end of the pharynx, resulting in a much shorter and unhindered displacement path.

The shorter displacement path has two beneficial effects

a) higher pumping rates are permitted, yielding a larger pumping capacity for a given lumen volume

b) the short displacement distance results in a much lower fluid velocity and therefore in less viscous energy loss.

Hence, it can be concluded that the longitudinally increasing pharynx is more efficient than the alternative, a radially increasing pharynx.

#### 4. The tapered pharynx

What arguments can be presented to account for the taper of the pharynx?

a) the taper of the lumen results in negative lumen pressures after the lumen starts closing. Thus, no regurgitation is possible, and the efficiency of pumping is increased.

b) diffusion limitations may also favor a tapered pharynx in large nematodes. The thick portion of the pharynx and the duct gland nuclei are close to the intestine, and therefore close to a higher concentration of metabolites. The concentration of metabolites at the anterior end of the pharynx will be lower if diffusion is the primary transport mechanism through this region of the pseudocoelom. Thus, if the availability of energy is the limiting factor to pharynx diameter, the anterior

region of the pharynx should be thinner. The open circles on Fig. 4-5 represent the maximum and minimum diameters for one Ascaris pharynx. The maximum and minimum values deviate significantly from the curve, however, the average diameter should fall close to the curve given by Roggen.

c) work as a function of the pumping sequence. The anterior segment of the pharynx must do work:

i) against the viscous forces of the lumen contents, and

ii) against the elastic forces of the pharynx. During relaxation no work is done on the lumen contents by the elastic forces. Therefore, elastic work done by the myofilaments in the contraction phase needs only be of a minimal nature.

The posterior segment of the pharynx must do work:

i) against the elastic structures of the pharynx

ii) against viscous forces in moving the lumen contents along the lumen

iii) a small amount of work is probably done in aiding the closing of the anterior region of the pharynx via negative pressure within the lumen. During relaxation the elastic components of posterior region of the pharynx must pressurize the lumen contents and finally move the contents into the intestine. The work done in contraction on the elastic components of the posterior region of the pharynx must be greater than those of the anterior region. Therefore, work considerations alone predict that the larger proportion of the muscle mass should be at the posterior end of the pharynx. That is, a tapered pharynx.

To conclude this section, the data and arguments presented support a tapered pharynx expanding posteriorly in the longitudinal direction for larger nematodes.

This concludes the discussion and development of the model pharynx. A general discussion and summary of Chapters 3 and 4 are the topic of Chapter 5.

CHAPTER 5

DISCUSSIONS AND CONCLUSION

A. General Discussion

Can the results of this study be applied more generally to the pharynges of other nematodes? The answer is yes, but with some reservations because Ascaris has a simple pharynx without specializations such as bulbs. Therefore, extrapolation of these conclusions to other nematodes must be confined to nonspecialized functions.

All pharynges have a triradiate lumen with radially oriented myofilaments. The mechanics of lumen opening via muscle contraction are probably very similar for all nematodes. In this study, it was shown by model analysis and measurement that myofilament shortening causes a pressure increase within the pharynx. The resulting pharyngeal dimensional changes were longitudinal in Ascaris, however there is no theoretical restriction which would prohibit radial changes. In general, one might find any (longitudinal strain)/(radial strain) ratio in a given nematode pharynx or region of the pharynx. However, it was shown that considerations of efficiency should favour a ratio greater than one in large nematodes.

All pharynges without bulbs could be expected to move the lumen contents by the peristalsis-like motion described for Rhabditis by Doncaster (1962). Peristalsis-like motion is the only method by which the simple cylindrical lumen may be closed at the anterior in order that the lumen contents may be pressurized above the nematode turgor pressure. Peristalsis-like motion would not be necessary in pharynges with median bulbs because this

configuration could operate successfully as a two-stage pump.

#### B. Future Extensions Of This Work

The possible cellular nature of the pharynx, as indicated by the failure of the action potential to propagate the full length of the pharynx, is an interesting problem which bears further investigation, especially in light of Reger's work (1966) showing intermembrane contacts. The cellular nature could be investigated by electrophoretically injecting the fluorescent dye, procion yellow, followed by fixation, embedding, and a fluorescence microscope study.

Another very interesting area of investigation would be the inter-relationship between central nervous system, pharyngeal enteric nervous system, and pharyngeal activity. The obvious method is via pharmacology and, in fact, some experiments were tried along these lines. The limitations of available time and the inconclusive and variable results caused this line of investigation to be abandoned. It was hoped to show whether it was the pharyngeal membrane or the enteric nervous system which was causing the spontaneous activity. Once this is established, the next question to be answered is how this activity is controlled in vivo? Presumably, by the central nervous system, but what is the stimulus?

The whole area of nematode electrophysiology is wide open. Only del Castillo and his co-workers have published any amount of work in the field, and of course, Ascaris is a good vehicle for this study because of its large size and ready availability. Some of this work

should be done on other nematodes as well, particularly free-living animals because of their small size and different habitat.

### C. Conclusions

The objective of this study was to investigate the operating principles of the nematode pharynx. This has been accomplished with some success, for the animal chosen - Ascaris lumbricoides.

The motion of the lumen is essentially peristaltic. Contraction of the radially oriented muscles open the lumen. The lumen opening causes a cytoplasmic pressure increase which results in changes in the pharynx external dimensions. During repetitive pumping, the dimensional changes are accomplished primarily via an average 15% longitudinal strain at the anterior end and considerably less longitudinal strain at the posterior end of the pharynx.

It was shown that these dimensional changes were insufficient to allow the lumen to open fully. The estimated maximum opening during repetitive pumping was approximately 70% of maximum cross-sectional configuration. This was equivalent to a triangular cross-section formed by the triradiate lumen. However, during maintained myofilament contraction, the lumen does open to the full circular configuration.

In order that the model exhibit the same dimensional changes as the isolated pharynx, the outer membrane could not be homogeneous, but was much less elastic in the circumferential direction. The ratio of the elastic constants  $E_{\psi}/E_{\ell}$  was equal to approximately

2.7. This was unexpected because the elastic properties of the lumen and marginal tissue, which constitute primarily longitudinal components, were included in the outer membrane of the model.

It was possible, through the use of the model, to account for the various observed dimensional changes for the pharynx by relating the myofilament force per unit area  $F_r$ , and pharynx pressure ( $P_p$ ). When  $F_r$  just exceeds  $P_p$  there is a positive radial strain. If  $F_r \approx 2P_p$ , the radial strain is zero. If  $F_r > 2P_p$ , a negative radial strain will be observed. At all times a longitudinal strain is observed in Ascaris pharynx in response to any pressure-induced stress.

It was shown that the volume of the pharynx in nematodes 100 mm and longer approaches a limit. This indicated that for large nematodes there may have been some evolutionary pressure for the selection of efficient pharynges. With this in mind, it was shown that a tapered, elongating pharynx was more efficient than other possible configurations, i.e., non-tapered radially increasing pharynges.

Three mechanisms were identified which would increase efficiency:

a) the primarily longitudinal strain results in less external work being done, displacing the pseudocoelom fluid during each pumping cycle.

b) the lumen contents are moved along the lumen by negative pressure at the posterior end rather than positive pressure at the anterior end. Therefore, any food ingested is pumped into the gut; no regurgitation is possible.



c) the average velocity of depolarization in the isolated pharynx was found to be  $4.0 \pm .20$  cm/sec whereas the velocity of repolarization was  $5.8 \pm .23$  cm/sec. This also has two beneficial effects:

i) it means that more time per pump is spent on intake of food. This could provide extra time for the ingestion of food through the narrow opening allowed by the tapering of the lumen.

ii) the rapidly advancing relaxation phase pressurizes the lumen contents quickly, minimizing any leakage back down the lumen.

It was found that the transmission of pressure along the pharynx occurs more slowly than the transmission of the action potential. Therefore, each section of the pharynx may be considered to act independently during muscle contraction.

To conclude, a mathematical model of the nematode pharynx has been constructed as a useful aid to the understanding of the various interrelated processes involved in making this organ function as a pump.

BIBLIOGRAPHY

- Allen, M.W., 1960. "Alimentary canal, excretory and nervous systems", in Nematology, (J.N. Sasser and W.R. Jenkins, eds), University of North Carolina Press, Chapel Hill, North Carolina.
- Bird, A.F., 1971. The Structure of Nematodes, Academic Press, New York.
- Bullock, T.H., and G.A. Holmes, 1965. Structure and Function in the Nervous System of Invertebrates, Volume 1, Freeman and Company, San Francisco.
- Büres, J., M. Petran, and J. Zachar (eds), 1960. Electrophysiological Methods in Biological Research, Academic Press, New York.
- Chitwood, B.G. and M.B. Chitwood, 1950. An Introduction to Nematology; "The esophagus including the esophago-intestinal valve", Chapter 6. Monumental Printing Company, Baltimore, Maryland.
- del Castillo, J. and T. Morales, 1967a. "The electrical and mechanical activity of the esophageal cell of Ascaris lumbricoides", J. Gen. Physiol., 50:603-629.
- del Castillo, J. and T. Morales, 1967b. "Extracellular action potentials recorded from the interior of the giant esophageal cell of Ascaris", J. Gen. Physiol. 50:631-645.
- del Castillo, J. and T. Morales, 1969. "Electrophysiological experiments in Ascaris lumbricoides", In Experiments in Physiology and Biochemistry, G.A. Kerkut, ed., 2:209-273.
- del Castillo, J., W.C. de Mello, and T. Morales, 1963. "The physiological role of acetylcholine in the neuromuscular system of Ascaris lumbricoides", Arch. Inter. de Physiol. et de Biochimie, 71:741-757.

- del Castillo, J., W. C. de Mello, and T. Morales, 1964. "Hyperpolarizing action potentials from the esophagus of Ascaris lumbricoides", Nature, London, 203:530-531.
- del Castillo, J., W.C. de Mello, and T. Morales, 1967. "The initiation of action potentials in the somatic musculature of Ascaris lumbricoides", J. Exp. Biol. 46:263-279.
- Doncaster, C.C., 1962. "Observations on Rhabditis and Peodera", Nematologica, 8:313-320.
- Goldschmidt, R., 1905. "Der chromidial Apparat lebhaft funktionierender Gewebszellen", Zool. Jb. Abt. Anat., 21:41-140.
- Hsü, H.F., 1929. "On the oesophagus of Ascaris lumbricoides", Z. Zellforsh. Anat., 9:313-326.
- Harris, J.E., and H.D. Crofton, 1957. "Structure and function in the nematodes: internal pressure and cuticular structure in Ascaris", J. Exp. Biol., 34:116-130.
- Hobson, A.D., W. Stephenson, and L.C. Beadle, 1952. "Studies on the physiology of Ascaris lumbricoides. 1. The relation of total osmotic pressure, conductivity and chloride of the body fluid to that of the external environment", J. Exp. Biol., 29:1-21.
- Katz, B., 1939. "The relation between force and speed in muscular contraction", J. Physiol., 96:45-64.
- Kobatake, Y., I. Tasaki and A. Watanabe, 1971. "Phase transitions in membrane with reference to nerve excitation", In Advances in Biophysics, 2:1-31.
- Lee, D.L., 1965. The Physiology of Nematodes. Oliver and Boyd, London.

- Mapes, C.J., 1965. "Structure and function in the nematode pharynx. I. The structure of the pharynges of Ascaris lumbricoides, Oxyuris equi, Aplectana brevicaudata, and Panagrellus silusiae", Parasitology, 55:269-284.
- Mapes, C. J., 1966. "Structure and function in the nematode pharynx. III. The pharyngeal pump of Ascaris lumbricoides", Parasitology, 56:137-149.
- Martini, E., 1916. "Die anatomie der Oxyaris curvula," Zeit. Wiss. Zool., 116:137-534.
- Mozgovoi, A.A., 1953. Essentials of Nematology, Volume 2, Part 1: Ascaridata of Animals and Man and the Diseases Caused By Them, The Academy of Sciences of the U.S.S.R., Moscow. Israel Program for Scientific Translations, Translated from Russian, 1968.
- Popova, T.I., 1958. Essentials of Nematology, Volume 7, Strongyloids of Animals and Man, The Academy of Sciences of the U.S.S.R., Moscow. Israel Program for Scientific Translations, Translated from Russian, 1965.
- Rapoport, S.I., 1971. "Velocity of action potential of frog muscle as a function of stretch and glycerol treatment", J. Gen. Physiol., 57:250-251.
- Reger, J.F., 1966. The fine structure of fibrillar components and plasma membrane in esophageal myoepithelium of Ascaris lumbricoides (var. suum), J. Ultrastruct. Res., 14:602-617.

- Roggen, D.R., 1970. "Is there an upper limit to the diameter of the pharynx in nematodes?", *Nematologica*, 16:605.
- Rosenbluth, J., 1967. "Obliquely striated muscle, III. Contraction mechanisms of Ascaris body muscle ", *J. Cell. Biol.*, 34:15-33.
- Skrjabin, K.I. (ed), 1954. Essentials of Nematology, Volume 3, Trichostrongyloids of Animals and Man, The Academy of Sciences of the U.S.S.R., Moscow; The Israel Program for Scientific Translations, 1960.
- Tasaki, I., E.H. Polley and F. Orrego, 1954. "Action potentials from individual elements in cat geniculate and striate cortex", *J. Neurophysiology*, 17:454.
- Turner, C.E., 1965. Introduction to Plate and Shell Theory, American Elsevier Pub. Co., New York.

CURRICULUM VITAE

NAME: James Richard Saunders

PLACE OF BIRTH: Duncan, British Columbia

DATE OF BIRTH: April 23, 1939

EDUCATION: University of Victoria, Victoria, B.C.  
Faculty of Arts and Science, 1961-1965.  
B.Sc. (Honours Physics), 1965.  
Simon Fraser University, Burnaby, B.C.  
Department of Biological Sciences  
Graduate Studies, 1969-1971.

EXPERIENCE: Laboratory Instructor, Department of  
Physics, University of Victoria,  
Victoria, B.C., 1964-1965.  
Assistant Master, Department of Physics,  
B.C. Institute of Technology,  
Burnaby, B.C., 1965-1969.  
Teaching Assistant, Department of  
Biological Sciences,  
Simon Fraser University, 1970-1971.  
Associate Master, Department of Physics,  
B.C. Institute of Technology,  
Burnaby, B.C., 1971-1972.